Expression and Purification of HIV-I TAT Protein Transduction Domain Fused with Acid β-glucosidase and Enhanced Green Fluorescent Protein

by

Andrea Kathleen Vaags
B.Sc., University of Victoria, 2000

A Thesis Submitted in Partial Fulfillment of the
Requirements for the Degree of

MASTER OF SCIENCE

in the Department of Biology

Supervisor: Dr. Francis Y. M. Choy

ABSTRACT

The protein transduction domain (PTD) of the HIV-I TAT protein has been shown to be capable of crossing cellular membranes and even the blood-brain barrier while carrying cargo molecules along with it. Exploiting this property to deliver biologically active acid β-glucosidase (GBA) would be of use to improve the current treatment of Gaucher disease by enzyme replacement therapy. Genetic fusion of the TAT PTD to GBA was performed and the resulting gene was inserted into an insect expression vector, p2ZOptcxF, to allow for heterologous protein production in *Sf*9 cells. A TAT fusion with enhanced green fluorescent protein (EGFP) was also created to serve as a control. The insect vector encoded a cellulose-binding domain to allow for affinity purification of the heterologous proteins. The *Sf*9 system produced 0.9-1.2 μg/ml quantities of EGFP fusion proteins, but only low ng/ml levels of GBA fusions. The addition of the cellulose binding domain decreased protein expression, but could be used for purification when μg/ml quantities of protein were produced. This suggests that expression of soluble, unglycosylated proteins such as EGFP can be achieved in the p2ZOptcxF/*Sf*9 system and to a lesser extent complex, highly-glycosylated proteins such as GBA can also be produced. In order to improve the expression of GBA fusions further optimization of the vector, selection and production must be undertaken.

TABLE OF CONTENTS

LIST OF TABLES

LIST OF FIGURES

LIST OF ABBREVIATIONS

%	percent
°C	degrees Celsius
4MU	4-methyl-umbelliferone
4MUGP	4-methyl-umbelliferyl-β-D-glucopyranoside
AIDS	Acquired Immune Deficiency Syndrome
BBB	blood-brain barrier
bp	base pairs
Ca^{+2}	calcium
CBD	cellulose binding domain
CBD_{Cex}	cellulose binding domain from *Cellulomonas fimi*
cDNA	complementary DNA
CHO	Chinese hamster ovary
cm	centimetre
CNS	central nervous system
COS-1	African green monkey kidney fibroblast cells
ddH_2O	deionized distilled water
DMSO	dimethyl sulfoxide
DNA	deoxyribonucleic acid
dNTPs	deoxynucleotide tri-phosphate
E. coli	*Escherichia coli*
egfp	enhanced green fluorescent protein gene
EGFP	enhanced green fluorescent protein
ERT	enzyme replacement therapy
et al.	*et alia*
FACS	fluorescence activated cell sorting
FITC	fluorescein isothiocyanate
gba	acid β-glucosidase (glucocerebrosidase) gene
GBA	acid β-glucosidase (glucocerebrosidase) protein
GD	Gaucher disease

GFP	green fluorescent protein
HeLa	Henrietta Lacks cervical carcinoma cells
HIV	Human immunodeficiency virus
HRP	horseradish peroxidase
HS	heparan sulfate
*ie*2	immediate early 2 promoter
kb	kilobase
kDa	kiloDaltons
kV	kiloVolts
LSLB	low salt Luria broth
LTR	long terminal repeat
Mg	microgram
µl	microlitre
µM	microMolar
mA	milliAmp
mg	milligram
ml	milliliter
mM	milliMolar
min	minute
mRNA	messenger ribonucleic acid
ng	nanogram
nm	nanometer
NMWL	nominal molecular weight limit
PCR	polymerase chain reaction
pmole	picomole
psi	pounds per square inch
PTD	protein transduction domain
PTD-4	modified protein transduction domain # 4
RFU	relative fluorescent units
RNA	ribonucleic acid
RT-PCR	reverse transcriptase polymerase chain reaction

s	second
SDS	sodium dodecyl sulfate
SDS-PAGE	sodium dodecyl sulfate polyacrylamide gel electrophoresis
*Sf*9	*Spodoptera frugiperda* IPLB-*Sf*21-AE cells
TAT	*trans*-activating transcriptional activator protein
TBS	Tris buffered saline
TTBS	Tris buffered saline with 0.05% Tween-20
UV	ultra-violet
v/v	volume per volume
w/v	weight per volume
x g	times gravity

ACKNOWLEDGEMENTS

I would like to thank my supervisor, Francis, for always maintaining a feeling of comraderie within the lab, for giving praise where it was deserved, and for his constant support and encouragement even in the face of disappointment. Thanks are due to my fellow lab mates; Judy Bandsmer, Agnes Zay, Laura Neilsen, Tessa Campbell, Graham Sinclair, Chelsea Patrick, Julie Wafaei, Natalie Devost, and Lisa Sharp for their advice and ability to keep it fun. Particular mention goes to the people who have worked side-by-side with me on this project: Judy Bandsmer, Jamie Haddon, Melissa Lem, Michelle Hubbard and Chelsea Patrick. For keeping me going and never doubting that I could succeed, I would like to thank my parents, family, and friends. Finally, I owe a great deal to Graeme Holfeld for his constant support and, as a wise man once wrote, for his "understanding that a half-hour of lab work actually means three"!

1 Introduction

1.1 Gaucher disease

1.1.1 Gaucher disease

Lysosomal enzymes are responsible for the turnover of a variety of molecules within the cell. Mutations within these enzymes result in over thirty inherited genetic disorders (Beutler *et al.*, 2001). One such disorder, Gaucher disease, results from mutations in the lysosomal enzyme acid β-glucosidase (previously known as glucocerebrosidase (EC 3.2.1.45)). Gaucher disease (GD) is an inherited, autosomal recessive disorder caused by decreased levels of active acid β-glucosidase (GBA). Common to all lysosomal storage disorders, the substrate of the defective enzyme accumulates within lysosomes. In the case of Gaucher disease, deficiency in GBA results in the buildup of glucosylceramide in the lysosomes of many cell types. Although GD is relatively rare, with an estimated incidence rate of 1:10000 (Beutler *et al.*, 1993), it is the most common lysosomal storage disorder.

1.1.2 Clinical manifestations

Gaucher disease is characterized by the deterioration of the organs, namely the spleen, liver, bone marrow and brain. The disease is usually classified into three subtypes: Type 1 (non-neuronopathic, adult), Type 2 (acute neuronopathic, infantile) and Type 3 (subacute neuronopathic, juvenile). All forms of Gaucher disease usually include organ and bone involvement. Type 1 Gaucher disease, the most common form, is found in all age groups and does not include brain/CNS involvement. Type 2 disease is found in

infants and involves severe mental retardation with a poor prognosis. Type 3 disease is found in children and young adults and includes mild to severe mental retardation.

One diagnostic hallmark of Gaucher disease is the presence of characteristic Gaucher cells, which are enlarged and lipid-laden due to the accumulation of glucosylceramide within the lysosomes. Glucosylceramide cannot be catabolized due to the lack of active GBA enzyme. These cells have been shown to be derived from the monocyte/macrophage system (Burns *et al.*, 1977), and have greatly elevated levels of glucosylceramide as macrophage cells collect and recycle membranes of cells.

1.1.3 Molecular Biology

The gene encoding the acid β-glucosidase (GBA) enzyme is 7604 base pairs (bp) in length and encodes eleven exons and ten introns (Horowitz *et al.*, 1989) on chromosome 1q21. Exons nine and ten encode the active site of the enzyme, and are the site of many mutations leading to a severe clinical phenotype (Ginns *et al.*, 1982; Van Weely *et al.*, 1991; Miao *et al.*, 1994; Fabrega *et al.*, 2000). The phenotypic heterogeneity of Gaucher disease can loosely be linked to the broad spectrum of mutations that occur within the gene for acid β-glucosidase (*gba*). In some instances, the severity of the disease has been correlated with the type of mutation present in the *gba* gene; the presence of the N370S mutation has been shown to preclude neurological involvement (Theophilus *et al.*, 1989), whereas L444P is strongly correlated with type 2 and 3 neuronopathic Gaucher disease (Strasberg *et al.*, 1994). More than 110 mutations have been identified (Horowitz *et al.*, 1994; Beutler *et al.*, 1998), the most common among Caucasian populations being N370S, L444P, R496H and 84GG (Beutler *et al.*, 2001), as well as many private

mutations that have only been found in one individual or family. The type of mutations found include single nucleotide substitutions, deletions, insertions, splice site abnormalities and recombinant alleles due to interaction with the *gba* pseudogene, which lies 16 kb downstream of the functional gene (Barranger *et al.*, 1995). The types of mutations present affect whether the mutated GBA enzyme is catalytically unstable, poorly activated or less thermostable (Barranger *et al.*, 1995).

1.1.4 Biochemistry

The defective enzyme in Gaucher disease is acid β-glucosidase (GBA), which is an acid hydrolase. This enzyme normally converts its substrate, N-acyl-sphingosyl-1-O-β-D-glucoside (glucosylceramide or glucocerebroside) to the products of glucose and ceramide (cerebroside), by hydrolysis of the β-glucosidic bond (Brady *et al.*, 1965a; Brady *et al.*, 1965b). GBA is a homomeric glycoprotein that in its native form is tightly associated with the membrane of lysosomes, yet no obvious basis for this association is evident from the primary sequence (Rijnboutt *et al.*, 1991). No transmembrane domains are present in the mature polypeptides, based on computer calculations. The mature polypeptide is 497 amino acids with a calculated molecular mass of 55,575 Daltons. The glycosylated enzyme from human placenta has a molecular mass of 65 kDa (Aerts *et al.*, 1987). High mannose and typical bi- and tri-antennary complex N-linked oligosaccharides are present on the human placental acid β-glucosidase (Takasaki *et al.*, 1984). GBA must be properly glycosylated at one of its five putative glycosylation sites to result in an active enzyme (Grace *et al.*, 1990a; Berg-Fussman *et al.*, 1993). Lack of

glycosylation of recombinant human GBA in bacteria or tunicamycin-treated insect cells results in a catalytically inactive enzyme (Van Weely *et al.*, 1991).

1.1.5 Enzyme Replacement Therapy

Historically, Gaucher disease (GD) could only be treated by the removal of the spleen or parts of the liver to decrease the load of Gaucher cells and accumulated glucosylceramide on the system. Eventually this type of treatment fails as the glucosylceramides accumulate in other body systems. Today, GD is treated not only by surgery but also with enzyme replacement therapy (ERT). ERT is the injection of active human placental (alglucerase) or recombinant (imiglucerase) acid β-glucosidase (GBA) into the bloodstream of GD patients. The injected enzyme has been modified to expose core α-mannosyl residues so that the macrophage mannose receptors will recognize and internalize the recombinant enzyme (Furbish *et al.*, 1981). This is accomplished by enzymatic removal of sialic acid, β-galactoside and N-acetyl-β-glucosamine residues. Once inside the macrophage, the enzyme enters the lysosomes where it is able to degrade the accumulated glucosylceramides (Hubbard *et al.*, 1979a; Hubbard *et al.*, 1979b). Despite the targeting of the recombinant enzyme to the macrophage, much of the injected enzyme is cleared from the body via breakdown in the liver (Beutler, 1997). Within the macrophage lysosomes of the liver and spleen, the enzyme has peak activity at 15-20 minutes, which rapidly decreases at 45-60 min (Xu *et al.*, 1996). Fifty percent visceral clearance is achieved in 1-2 hours, with the other half disappearing between 12-42 hours; in bone marrow the $t_{1/2}$ is about 14 hours (Mistry *et al.*, 1996; Friedman *et al.*, 1999). Due

to the short half-life of administered enzyme, ERT must be performed on a bimonthly basis to keep the levels of glucosylceramide in check.

Another limitation of ERT is that the injected enzyme is not able to cross the blood-brain barrier (BBB) and thus is not able to degrade accumulated substrate within the brain. Proteins in excess of 700 Daltons do not typically enter into neural cells, making treatment of neurological disorders via protein therapeutics unfeasible (Scheld, 1989; Egleton *et al.*, 1997). As the cost of ERT is $100,000 to $300,000 US per year for a typical adult patient (Weinreb *et al.*, 2002), ERT is not normally employed on Type II and III patients who have severe neurological involvement (Brady *et al.*, 1997). This limitation of ERT has prompted research into overcoming the impenetrable BBB; in our case, through the use of a recombinant fusion enzyme containing a protein transduction domain to facilitate trans-membrane delivery.

1.2 Trans-membrane Protein Transduction

An expanding area of research is the field of cell-penetrating peptides, and their use as delivery agents for proteins, nucleic acids, liposomes, and nanoparticles. Such cell-penetrating peptides are of particular interest for the delivery of therapeutics to treat a variety of human diseases. Preliminary work has been done on HIV-AIDS (Vocero-Akbani *et al.*, 1999), diabetes (Embury *et al.*, 2001), ischemic brain injury (Cao *et al.*, 2002; Dietz *et al.*, 2002; Kilic *et al.*, 2003), and Mucopolysaccharidosis VII (Elliger *et al.*, 2002). This thesis focuses on the use of one particular cell-penetrating peptide, HIV TAT, and its potential use as a delivery agent for acid β-glucosidase enzyme replacement therapy.

1.2.1 Known Transducing Proteins

Protein transduction domains (PTDs) are portions of naturally occurring proteins that have the ability to cross cellular membranes. Several PTDs have been identified including those from the antennapedia protein of *Drosophila melanogaster* (Derossi *et al.*, 1994), the chimeric peptide transportan (Pooga *et al.*, 1998), the Herpes simplex virus-I VP22 (Bennett *et al.*, 2002), as well as the HIV-I *trans*-activating transcriptional activator (TAT) protein (Frankel *et al.*, 1988; Fawell *et al.*, 1994). All of these proteins have a strong basic character and are rich in arginine residues, yet they share little sequence or structural homology (Futaki *et al.*, 2001; Zhao *et al.*, 2004). Several studies using these peptides have demonstrated highly efficient delivery into cells both *in vitro* and *in vivo* (Fawell *et al.*, 1994; Schwarze *et al.*, 1999; Ferrari *et al.*, 2003; Mie *et al.*, 2003).

1.2.2 The HIV TAT Protein

The HIV TAT protein is expressed by the Human Immunodeficiency Virus type I as an 86 amino acid protein. This protein is expressed early in the HIV infection and binds to the 5' long terminal repeat (LTR) of the initial viral mRNA transcript and induces the synthesis of viral RNA and protein (Arya *et al.*, 1985; Sodroski *et al.*, 1985; Varmus, 1988; Frankel *et al.*, 1998). The TAT protein also has other activities, including cell growth stimulation (Ensoli *et al.*, 1993) and trans-cellular transactivation (Frankel *et al.*, 1988; Frankel *et al.*, 1989), when it is released in an extracellular form from infected cells.

In 1988, both Green and Lowenstein and Frankel and Pabo , independently reported that externally applied HIV-TAT was able to stimulate HIV-LTR-driven RNA synthesis in intact cells. They did not demonstrate directly that the TAT protein was transduced into the cytosol and nucleus, though it appeared to be very likely.

The TAT protein is composed of six domains; the acidic (residues 2-11) and cysteine-rich (residues 22-37) regions, the hydrophobic core (residues 38-48), the basic (residues 49-57) and the glutamine-rich (residues 58-72) regions, and the RGD motif (residues 72-86) (Bayer *et al.*, 1995). The basic region is required for binding of the protein to the negatively-charged, initial mRNA viral transcript to allow for further transcription (Weeks *et al.*, 1990; Churcher *et al.*, 1993; Kempf *et al.*, 2002). This basic region is also responsible and sufficient for the translocating properties of the TAT protein (Vives *et al.*, 1997a).

1.2.3 The Protein Transduction Domain of HIV-I TAT

In 1994, Fawell *et al.* determined that a 36 amino acid domain of the TAT protein, when chemically cross-linked to cargo proteins, was able to transduce into cells . It was the work of Vives *et al.* (1997a) that demonstrated that an even smaller domain of the TAT protein, extending from amino acid residues 47-58, had this transducing ability. Dowdy and coworkers developed genetically conjugated proteins using a similar segment of residues, amino acids 47-57, to achieve transduction of heterologous proteins (Ezhevsky *et al.*, 1997). A variety of authors have indicated that the protein transduction domain (PTD) can be added to a fusion protein partner, to allow for transport of the protein partner into cells (Fawell *et al.*, 1994; Nagahara *et al.*, 1998; Schwarze *et al.*,

1999; Vocero-Akbani *et al.*, 1999; Dowdy, 2000; Park *et al.*, 2000; Vocero-Akbani *et al.*, 2000; Becker-Hapak *et al.*, 2001; Embury *et al.*, 2001; Ho *et al.*, 2001; Morris *et al.*, 2001; Vocero-Akbani *et al.*, 2001; Cao *et al.*, 2002; Dietz *et al.*, 2002; Ferrari *et al.*, 2003; Kilic *et al.*, 2003; Mie *et al.*, 2003; Vazquez *et al.*, 2003; Wheeler *et al.*, 2003; Ziegler *et al.*, 2003; Zhao *et al.*, 2004).

This small peptide of eleven amino acids has many basic (arginine and lysine) residues and is denoted as the protein transduction domain (PTD). The PTD is thought to form an α-helix with the amphipathic amino acids aligned along one side of the helix (Ho *et al.*, 2001). Addition of the PTD to either the N- or C-terminus is possible (Fawell *et al.*, 1994; Silhol *et al.*, 2002), although some work has shown that C-terminus addition is necessary to have the protein of interest secreted from cells and thus allow for inter-cellular transduction (Elliger *et al.*, 2002). The TAT peptide is highly hydrophilic and as such causes very little disturbance to the plasma membrane of cells even at concentrations as great at 100 μM (Hallbrink *et al.*, 2001). Unlike other proteins with transduction activity the TAT peptide has very low toxicity in cell culture (Vives *et al.*, 1997a; Hallbrink *et al.*, 2001).

1.2.4 Modified TAT Protein Transduction Domain

Researchers have attempted to modify the form of the HIV TAT PTD so as to increase the efficiency of its transduction capabilities (Wender *et al.*, 2000; Ho *et al.*, 2001). Work done by Ho *et al.* (2001), modeled the structure of the TAT PTD as a strong amphipathic helix, and synthetic PTDs with a strengthened alpha-helical character as well as optimized placement of arginine residues resulted in enhanced transduction activity.

By aligning basically-charged arginine residues on one face of the predicted alpha-helix and substituting alpha-helical-promoting alanine residues opposite the arginine face, the transduction ability of the TAT PTD was increased as much as 33 times above that of the native PTD. This most efficient synthetic peptide (PTD-4) was chosen to be employed in our work so as to further increase the chance of transduction of the fusion protein partner.

1.2.5 Mode of Cellular Transduction

A topic of intense debate is how TAT proteins and PTDs are transported across cellular membranes into the cytosol and the nucleus. To date, the exact mechanism of membrane translocation remains unknown.

Electrostatic attraction between opposite charges of the positively-charged TAT PTD and negatively-charged cellular membranes may play a role in translocation (Silhol *et al.*, 2002; Richard *et al.*, 2003; Ziegler *et al.*, 2003). The structural properties of the numerous positively-charged arginine residues within the peptide have been thoroughly examined using several chemical analogs. These studies looked at amino acid chirality (Wender *et al.*, 2000), the guanidine head group (Wender *et al.*, 2000; Suzuki *et al.*, 2002), alkyl side chain (Wender *et al.*, 2000), and peptide backbone (Wender *et al.*, 2000; Suzuki *et al.*, 2002; Tung *et al.*, 2002). Overall, it was found that the translocating activity of the TAT peptide is largely due to the high density of guanidine groups (arginine), and that the other structural properties contribute little or no effect (Wender *et al.*, 2000; Rothbard *et al.*, 2002; Suzuki *et al.*, 2002).

During the 1990's, it was thought by some (Derossi *et al.*, 1996; Vives *et al.*, 1997a) that translocation occurred in an energy-independent manner as it occurs even at

4°C, a temperature that abolishes active transport mechanisms involving endocytosis (Vives *et al.*, 1997a). Yet in 1991, Mann and Frankel published an often overlooked article that demonstrated uptake of TAT by endocytosis, an ATP-requiring process, and that cells contain $>10^7$ binding sites/cell, although they were unable to identify a specific receptor . More recently, it has been demonstrated that sodium azide, which inhibits energy-dependent cellular uptake (Sandvig *et al.*, 1982), also inhibits the uptake of the TAT-PTD. This indicates that the transport of tat peptides is indeed energy-dependent (Wender *et al.*, 2000). Yet according to Silhol *et al.* (2002), endocytosis does not seem to be a requirement for entry of TAT peptides and their conjugates, but is for the full-length TAT protein.

Although it continues to be suggested by Derossi *et al.* (1996) and Vives *et al. (1997b)* that the TAT- PTD is transduced in a receptorless fashion, two laboratories demonstrated in 1993 that TAT and the TAT-PTD bind to specific cell surface proteins called integrins, indicating that delivery may be receptor mediated (Vogel *et al.*, ; Weeks *et al.*). TAT also binds to the lipoprotein receptor-related protein in neuronal cells (Liu *et al.*, 2000), and the receptors for vascular endothelial growth factors (Albini *et al.*, 1996b). Recently, heparan sulfate (HS) has become a major contender for mediating TAT cell-surface binding and internalization (Albini *et al.*, 1996a; Tyagi *et al.*, 2001). TAT and the PTD can be taken up by various tissue types, which suggests that a conserved cell membrane determinant or receptor is responsible for internalization. Interestingly, work has shown that HS may be needed for transduction of the full-length TAT protein, but not for the PTD. Tyagi *et al.* (2001) published convincing biochemical and genetic evidence that cell surface HS proteoglycans are responsible for the internalization of the full-length

TAT protein fused to glutathione S-transferase or green fluorescent protein. Work done by Silhol *et al.* (2002) later demonstrated that this may be true for the full-length TAT protein but that the TAT-PTD does not require HS or endocytosis and must use an as yet unknown mechanism for internalization.

Adding to the debate, recent research has shown that full-length TAT and TAT-PTD internalization occurs through a caveolar lipid-raft endocytic pathway for HeLa, Cos-1, CHO and HL3T1 cells (Ferrari *et al.*, 2003; Fittipaldi *et al.*, 2003) and not through the clathrin-coated pits as was demonstrated for full-length TAT in T cells (Vendeville *et al.*, 2004). Unfortunately all of these studies, except for Ferrari *et al.* (2003), employed fluorescence-activated cell sorting (FACS) and immunofluorescence microscopy of fixed cells, which may complicate the interpretation of their results.

Many studies on the translocation of proteins from the cell exterior to the nucleus have used the techniques of cell fractionation, FACS, or immunofluorescence of fixed cells (Fawell *et al.*, 1994; Bonifaci *et al.*, 1995; Vives *et al.*, 1997a; Nagahara *et al.*, 1998; Vocero-Akbani *et al.*, 1999; Park *et al.*, 2000; Vocero-Akbani *et al.*, 2000; Becker-Hapak *et al.*, 2001; Embury *et al.*, 2001; Fujiwara *et al.*, 2001; Morris *et al.*, 2001; Vocero-Akbani *et al.*, 2001; Silhol *et al.*, 2002; Wheeler *et al.*, 2003; Vendeville *et al.*, 2004). These methods have the potential for problems with misinterpretation, as cell fractionation or fixation may allow association of proteins with the nucleus or cytoplasm after the cells are disrupted, whereas FACS is unable to differentiate between surface-bound and internalized TAT proteins. As the TAT PTD contains stretches of positively charged amino acids, the affinity of these regions for the cell surface and nuclei may be a problem after membrane disruption (Olsnes *et al.*, 2002). With immunofluorescence

experiments it is common for the cells to be permeabilized with methanol, ethanol or paraformaldehyde (Derossi *et al.*, 1996; Tyagi *et al.*, 2001; Silhol *et al.*, 2002) to allow fluorescently labeled antibodies to interact with the protein of interest. Because the fixation may damage intracellular diffusion barriers, proteins that were located on the cell surface or inside membrane-bounded vesicles in the living cell may diffuse into the cytosol or nucleus during the fixation period (Olsnes *et al.*, 2002). Thus work done by groups such as Wender *et al.* (2000), Mie *et al.* (2003), Ferrari *et al.* (2003) and Vazquez *et al.* (2003) which study transduction on live cells using pre-labeled fluorescent proteins are superior, and may indicate, overall, an energy-dependent, cell surface determinant-mediated transduction of the TAT-PTD and its fusion partners.

1.2.6 HIV-I TAT PTD Transduction across the Blood-Brain Barrier

As early as 1994, Fawell *et al.* demonstrated *in vivo* distribution of TAT fusion proteins within mice. This work showed fusion proteins localized to liver, spleen and heart, as well as to the lung and skeletal muscle in low levels, but showed no localization to the brain . Later, Schwarze *et al.* (1999) showed that intraperitoneal injection of the 120 kDa β-galactosidase protein fused to the TAT-PTD resulted in delivery of biologically active fusion protein into blood, splenic, liver, kidney, lung, heart, skeletal muscle and brain cells. Demonstration that the BBB remained intact during the transduction process, increased excitement over the possible therapeutic utility.

Recently, Cao *et al.* (2002) and Kilic *et al.* (2002) have independently delivered Bcl-X_L to the brains of mice, where it acts to decrease cerebral infarction, increase the number of viable neurons and reduce the number of caspase-3-immunoreactive cells after

focal ischemia. Kilic *et al.* (2003) have also used a TAT-glial line-derived neurotrophic factor fusion to further protect from focal cerebral ischemia.

1.3 Expression System

For this study an insect expression system was employed to produce the TAT-tagged proteins. *Spodoptera frugiperda* (*Sf*9) cells and a stable expression insect vector were employed. The vector encodes a human transferrin secretion signal to direct the recombinant proteins to the medium, a cellulose-binding domain to allow affinity purification, and a Zeocin™ resistance gene to allow selection of stable insect clones.

1.3.1 Spodoptera frugiperda (Sf9) cells

*Sf*9 cells are a clonal isolate derived from *Spodoptera frugiperda* IPLB-Sf21-AE cells of the fall armyworm insect. This Lepidopteran cell line is employed for the transient or stable production of recombinant proteins. *Sf*9 cells, like other eukaryotic cells, covalently modify many of their proteins by N-glycosylation. The complexity of insect protein N-glycosylation is intermediate between those of *Saccharomyces cerevisiae* and mammalian cells. In all three systems a common intermediate, $Man_8GlcNAc_2$-N-Asn, is produced but it is converted to distinct end products (Altmann *et al.*, 1999; Staudacher *et al.*, 1999). In insect cells, exoglycosidases and a glycosyltransferase catalyze trimming and elongation reactions which yield $GlcNAcMan_3GlcNAc_2$-N-Asn, which is then converted to $Man_3GlcNAc_2$-N-Asn by an exoglycosidase that removes the terminal N-acetylglucosamine residue (Hollister *et al.*,

2002). In general, insect cells are incapable of producing complex, terminally-sialylated N-glycans, which are produced by mammalian cells.

Hollister *et al.* (2002) have shown that transgenic *Sf*9 cells can be manipulated to express mammalian genes encoding functions that are missing or limited, relative to mammalian cells. They suggest that the addition of constitutively expressible mammalian β4Gal-T, α2,6-sialyltransferase (ST6GalI) and glycosyltransferase GlcNAc-TII, allow *Sf*9 cells to produce extensively processed, biantennary, terminally sialylated N-glycans. A *Sf*9 related cell line, *Trichoplusia ni*, has recently been modified by Tomiya *et al.* (2003) to produce human transferrin with complex biantennary N-glycans. The use of such a transgenic *Sf*9 cell line for the expression of human proteins, such as GBA, warrants further exploration. Nonetheless, previous work in our laboratory has shown that the wildtype *Sf*9 system is capable of producing an active recombinant human GBA protein, that is glycosylated though presumably not terminally sialylated (Sinclair, 2001).

1.3.2 The p2ZOptcxF vector

All expression was done using the p2ZOptcxF (T. Pfeifer, University of British Columbia, Vancouver, BC) vector constructed from the p2Zop2F backbone by Hegedus *et al.*(1998). This vector is one of a series of shuttle vectors constructed to allow expression of heterologous proteins in either dipteran or lepidopteran insect cell lines. The expression of foreign proteins in insect cell lines has been dominated by derivatives of the Lepidopteran baculovirus, *Autographa californica* multicapsid nucleopolyhedrosis virus (AcMNPV) (Luckow *et al.*, 1989; Maeda, 1989), but the lytic nature of the AcMNPV infection markedly disrupts the cells' protein processing machinery

(Chazenbalk *et al.*, 1995). Proteins localized to the nucleus or cytoplasm are usually expressed at high levels using AcMNPV infection, but those entering the secretory pathway associated with the endoplasmic reticulum are often expressed in lower quantities (Jarvis, 1993; Jarvis *et al.*, 1996). As the proteins expressed in this work were desired to be produced in high quantities and secreted to the medium, the use of a constitutively active expression vector with a secretion signal, such as that of the p2ZOptcxF vector, rather than Baculovirus infection was indicated.

1.3.2.1 The OpMNPV ie2 promoter

Constitutive protein expression in a broad range of host cells can be mediated by the *Orgyia pseudotsugata* multicapsid nucleopolyhedrosis virus (*Op*MNPV) immediate-early (*ie2*) promoter. Genes under the control of this promoter are transcribed early after infection or transformation. Expression is detectable at 0.5 hours post-infection and reaches peak steady-state levels by 6 hours (Theilmann *et al.*, 1992). Pfeifer *et al.* (1997) demonstrated effective functioning of the *ie2* promoter in both dipteran and lepidopteran cell lines for the expression of a Zeocin™ resistance gene. A variety of human proteins have since been successfully expressed under the direction of the *ie2* promoter (Li *et al.*, 2001; Kempf *et al.*, 2002; Morais *et al.*, 2003).

1.3.2.2 Human transferrin secretion signal

The p2ZOptcxF vector uses the human transferrin secretion signal of the transferrin serum subtype. The secretion signal is 19 amino acids in length and has a sequence of MRLAVGALLVCAVLGLCLA (one letter amino acid code). The secretion

signal directs the protein to exit the cell and is cleaved once the protein is secreted. Work by Ali *et al.* (1996) has shown that this secretion signal is effective at directing proteins to the supernatant in *Trichoplusia ni* insect cell culture, which is also of the Lepidopteran family.

1.3.2.3 Cellulose binding domain

An N-terminal cellulose binding domain (CBD_{Cex}) sequence from the bacterium *Cellulomonas fimi* is located in the p2ZOptcxF vector after the human transferrin secretion signal. This domain has been added to act as an affinity tag for purification of the protein of interest. Cellulose binding domains (CBDs) are discrete protein regions found in a large number of carbohydrolases. The CBD_{Cex} belongs to family II of cellulose binding domains (Gilkes *et al.*, 1991; Tomme *et al.*, 1998), is 108 amino acids in length and binds strongly and specifically to crystalline cellulose (Creagh *et al.*, 1996; Tomme *et al.*, 1996; Tomme *et al.*, 1998). The CBD_{Cex} is natively found at the C-terminus of the glucanase, but is expressed at the amino-terminus of our target proteins. Ong *et al.* (1989) have shown that this domain could be effective when added at either terminus.

The use of a cellulose-binding domain is desirable because the cellulose affinity matrix is inexpensive, inert, stable under steam sterilization or caustic cleaning, and readily available in different forms including paper, fibres, powders and membranes (Assouline *et al.*, 1993). Additionally, CBDs do not affect the activity of the fusion partner (Greenwood *et al.*, 1989; Ong *et al.*, 1989), and can be desorbed from cellulose with (Wassenberg *et al.*, 1997) or without (Ong *et al.*, 1989) the use of counter ligands. Work by Guarna *et al.* (2000), Ong *et al.* (1991; 1993) and Assouline *et al.* (1993) have

shown that CBD_{Cex} fusion proteins can be eluted from cellulose by washing with large quantities of distilled water. After purification on cellulose, the CBD_{Cex} can be removed due to the addition of a factor X_a cleavage signal added at the C-terminus of the CBD. This protease cleaves at the C-terminus of its recognition site, which liberates the target protein without extraneous amino acids. The affinity tag can then be removed from the purified protein by adsorption on the cellulose affinity matrix used to purify the fusion protein (Assouline *et al.*, 1993; Assouline *et al.*, 1995).

1.3.2.4 Zeocin™ resistance

Zeocin™ is a member of the bleomycin/phleomycin family of antibiotics isolated from *Streptomyces cerevisiae*, which acts by cleaving host cell DNA. It is active against bacteria and higher eukaryotic cell lines, allowing the use of only one drug resistance marker for selection in both *E.coli* and *Sf*9 cells. The Zeocin™ resistance protein is designated *Sh ble* (*Streptoalloteichus hindustanus* bleomycin) and is 13,665 Daltons in mass. *Sh ble* binds to Zeocin™ in a stoichiometric manner and thereby inhibits DNA cleavage by the antibiotic (Calmels *et al.*, 1991). In the p2ZOptcxF vector, antibiotic resistance is driven by a chimeric ie2- EM7 bacterial synthetic promoter (Hegedus *et al.*, 1998).

1.4 Green Fluorescent Protein

In order to easily identify proteins expressed by the insect expression system, green fluorescent protein was employed as a control. The enhanced green fluorescent

protein variant was employed to allow for visualization with FITC filters on an epi-fluorescence microscope.

1.4.1 Green fluorescent protein

Shimomura *et al.* first discovered green fluorescent protein (GFP) in the jellyfish, *Aequoria victoria*, in 1962 . It was observed that the jellyfish was capable of emitting green fluorescent light when it was disturbed. The green fluorescent protein was cloned and characterized by Prasher *et al.* in 1992 .

GFP is 238 amino acids in length and is encoded by three exons that span a region of 2.6 kilobases (kb). The protein contains a hexapeptide structure that is known as the chromophore region. The hexapeptide is constituted by the amino acid sequence Phe-Ser-Tyr-Gly-Val-Gln, and the functional portion is formed by cyclization of Ser-dehydroTyr-Gly (Cody *et al.*, 1993).

In vivo light production from this protein occurs when energy, in the form of blue light, is transferred from a Ca^{+2}-activated photoprotein, aequorin, to the chromophore of GFP causing cyclization of Ser-dehydroTyr-Gly and the release of a lower energy photon of green light (Morise *et al.*, 1974). *In vitro* light production can occur without aequorin, by the direct illumination of GFP with blue light.

1.4.2 The enhanced green fluorescent protein variant

The enhanced GFP mutant (EGFP) is a human codon-bias optimized (Yang *et al.*, 1996) green fluorescent protein (GFP) constructed from the GFPmut1 produced by Cormack *et al* (1996). This mutant was selected because it has an absorbance that has

been shifted from the wild-type absorbance of 395 nm to 488 nm. EGFP is thus said to be red shifted, which is useful as the typical illumination range of equipment used for detecting fluorescence is between 450 and 500 nm. EGFP has the advantage of more intense fluorescence (Cormack *et al.*, 1996) and more rapid cyclization of the chromophore, but also has limitations that are not present in the wild type GFP. Although EGFP is able to produce fluorescence more rapidly after excitation with 488 nm light, it does not have enhanced stability of the cyclized chromophore and thus exhibits twofold faster photobleaching than wild-type GFP (Patterson *et al.*, 1997). Photobleaching is the phenomenon whereby a fluorescent signal is quenched by extended excitation over time, necessitating that images of the EGFP tagged proteins be taken quickly (within 2-3 minutes) after initial excitation with blue light, before the EGFP chromophore becomes unstable and has decreased fluorescence emission (Patterson *et al.*, 1997).

1.5 Main Objectives

This work focuses on the production of TAT fusion proteins that may have enhanced trans-membrane and trans-blood-brain barrier delivery compared to that of untagged proteins. Production of fusion proteins was carried out in eukaryotic *Sf*9 insect cells and purification was aided by the addition of a cleavable cellulose-binding domain affinity tag. EGFP proteins tagged with TAT were employed as a control, to demonstrate the utility of the expression and purification systems. GBA proteins fused to the TAT domain were intended for use in transduction studies to demonstrate the potential use of a TAT fusion protein with biological activity within cells, as an enhancement to the current proteins used for enzyme replacement therapy of Gaucher disease.

2 Materials and Methods

2.1 Chemicals, Reagents, and Equipment

The following were obtained from commercial sources:

ACP, Montreal, QC: KCl, $MgSO_4$-$7H_2O$. *Amersham, Piscataway, NJ*: Easy Breeze™ gel-drying apparatus, ECL+ chemiluminescent reagent and Hybond-P PVDF membrane. *BDH Inc., Toronto, ON*: $MgCl_2$-$6H_2O$. *Becton, Dickinson and Company, Sparks, MD*: tryptone, yeast extract. *Bio/Can Scientific, Mississauga, ON*: 10X UltraTherm™ polymerase buffer, $MgCl_2$, and UltraTherm™ polymerase. *Biotek, Winooski, VT*: Synergy HT-I microtitre plate reader and KC4 software. *BioRad Laboratories, Hercules, CA*: 0.1 cm gap cuvettes, 40% acrylamide/2% bis-acrylamide solution, BioRad Protein Assay, GenePulser electroporation machine and Mini-Protean II Electroblot Apparatus. *Carl Zeiss Canada Ltd., North York, ON*: IIIRS epi-fluorescence condenser, 490/525 nm FITC fluorescence filter #48 77 09, HBO-50 Universal Arc Fluorescent lamp, and Universal Compound Microscope. *Clontech, Palo Alto, CA*: pEGFP-N1 vector, recombinant EGFP protein, and Living Colors™ Anti-EGFP antibody. *DNASTAR, Madison, WI*: SeqMan™ software. *Eastman Kodak, Rochester, NY*: BioMax MR film, Triton X-100. *EM Science, Merck KGaA, Darmstadt, Germany*: agarose, $NaCl_2$, $(NH_4)_2SO_4$. *EMD Biosciences, San Diego, CA*: Factor X_a, monoclonal anti-CBD antibody and Novagen Factor X_a Cleavage Capture kit. *Fisher Scientific, Fair Lawn, NJ*: ethidium bromide, FisherFinest glass slides, $MgSO_4$ and Tween-20. *Fuji Photo Film, Tokyo, Japan*: FinePix 990 digital camera. *Invitrogen Canada, Burlington, ON*: 3X SDS-PAGE loading buffer, Cellfectin™ lipofection reagent, DNA 1 kb ladder, dNTPs, Sf900II SFM media, Superscript II Reverse Transcriptase, Superscript II First-strand Synthesis Kit, and

Zeocin™ antibiotic. *Kendro Laboratory Products, Ashville, NC*: RC 26 Plus ultracentrifuge and Sorvall SS34 rotor. *Media Cybernetics, San Diego, CA*: Image-Pro Plus analysis software. *Microsoft Canada Co, Mississauga, ON*: Excel software. *Millipore, Billerica, MA*: 10,000 NMWL polyethersulfone membrane, Amicon stirred cell apparatus, and Ultra-free 4 centrifugal concentrator. *New England Biolabs, Beverly, MA*: 10X T4 DNA ligase buffer, bovine serum albumin, Broad Range Protein standard, Calf Intestinal Phosphatase, EcoRI, NEBuffer EcoRI, NEBuffer 2, T4 DNA ligase and XbaI. *Owl Separation Systems, Portsmouth, NH*: Emperor Penguin™ Dual Gel Vertical Electrophoresis System. *Pall Corporation, East Hills, NY*: 30,000 NMWL Nanosep™ centrifugal devices. *Perkin Elmer, Wellesley, MA*: GeneAmp PCR thermal cycler. *Qiagen, Missassauga, ON*: DNeasy Tissue Kit, Qiaprep Miniprep kit, Qiaquick PCR purification kit, RNase-Free DNase set, and RNeasy Mini Kit. *Qiagen Operon, Missassauga, ON*: custom primers, oligo-$(dT)_{15}$ primer. *Roche, Indianapolis, IN*: phenylmethylsulfonyl fluoride, Tris base. *Sigma-Aldrich Canada, Oakville, ON*: 0.4% trypan blue, 4-methyl-umbelliferone, 4-methyl-umbelliferyl-β-D-glycopyranoside, dimethyl sulfoxide, rabbit anti-mouse horseradish peroxidase conjugated antibody, Sigmacell™ cellulose. *Stressgen, Victoria, BC*: goat anti-rabbit horseradish peroxidase conjugated antibody.

2.2 Expression Vector Construction

2.2.1 PCR amplification of DNA inserts using Pfu polymerase

All DNA inserts were amplified with *Pfu* polymerase chain reaction (PCR) using 1X *Pfu* buffer (20 mM Tris base, pH 7.5, 10 mM KCl, 10 mM $(NH_4)_2SO_4$, 2 mM $MgSO_4$,

1% (v/v) DMSO, 0.1% (v/v) TRITON X-100), 0.25 mM dNTPs (Invitrogen Canada, Burlington, ON), 0.6 μM sense and anti-sense custom primers (Qiagen Operon, Mississauga, ON) and 0.5 units of *Pfu* polymerase (donation from Dr. D. Levin, University of Victoria, Victoria, BC). Amplification was done on a GeneAmp PCR thermal cycler (PerkinElmer, Wellesley, MA) with an initial 94°C denaturation for 2 minutes, followed by 30 cycles of 1.5 minutes denaturing at 94°C, 1.5 minutes primer annealing at 50-60°C, and 2 minutes for primer elongation at 72°C. A final period of elongation at 72°C was carried out for 5 minutes. Primer information is described in Table 2.1 and a diagram of the vectors created is in Figure 2.1.

To create recombinant plasmids containing the *gba* insert, the *gba* cDNA from pFastBac-GBA (donation from Dr. G. Sinclair, University of British Columbia, Vancouver, BC) was PCR-amplified with primers G1 and G2, which both include *Eco*RI RE cut sites to allow for cloning into the vector. Subsequently, this 1558 base pair (bp) fragment was digested, purified, and cloned in-frame with the secretion signal of the p2ZoptcxF vector (donation from Dr. T. Pfeifer, University of British Columbia, Vancouver, BC; see Figure 2.1) to create p2ZOptcxF-GBA.

To create the recombinant plasmid containing the TAT sequence followed by *gba*, PCR- amplification using primers G3 and G2 was carried out with pFastBac-GBA as template. Primer G3 encodes an *Eco*RI cut site, the entire sequence of TAT and 15 bp of the 5' end of exon 3 of the *gba* gene. In conjunction with the reverse primer G2, a 1595 bp DNA fragment was created which was digested, purified and cloned-in frame with the secretion signal of p2ZOptcxF, to create p2ZOptcxF-TAT-GBA. In a similar manner, primers G4 and G2 were employed to produce a recombinant plasmid containing the

Table 2.1. Primers utilized for amplification of GBA, TAT-GBA, PTD4-GBA, EGFP, and PTD4-EGFP inserts to be cloned into p2ZOptcxF vector.

Primer[a]	Sequence[b] (5' to 3')	Orientation
G1	TAT**GAATTC**GCCCGCCCCTGCATCCCT	Sense
G2	GCGG**GAATTC**TTTAATGCCCAGGCTGAGCC	Anti-sense
G3	C**GAATTC**TACGGCCGCAAGAAACGCCGCCA GCGCCGCCGCGGTGGAGCCCGCCCCTGCAT	Sense
G4	C**GAATTC**TACGCCCGCGCGGCAGCCCGCCAG GCACGCGCAGGTGGAGCCCGCCCCTGCAT	Sense
E1	AACGGTC**GAATTC**ATGGTGAGCAAGGG	Sense
E2	TATGATCT**GAATTC**GCGGCCGCTTTACTT	Anti-sense
E3	TT**GAATTC**TACGCACGAGCAGCAGCACGCCAG GCACGAGCAGGTGGAGTGAGCAAGGGCGAG	Sense

[a]Primers G1 and G2 were used to create a GBA cDNA insert. Primers G3 and G2, and G4 and G2 were used to create a GBA cDNA insert with a N-terminal TAT or PTD4 cDNA, respectively. Primers E1 and E2 were used to create an EGFP cDNA insert. Primers E3 and E2 were used to create an EGFP cDNA with a N-terminal PTD4 cDNA.

[b]Nucleotides introduced to create restriction enzyme recognition sites are presented in bold print.

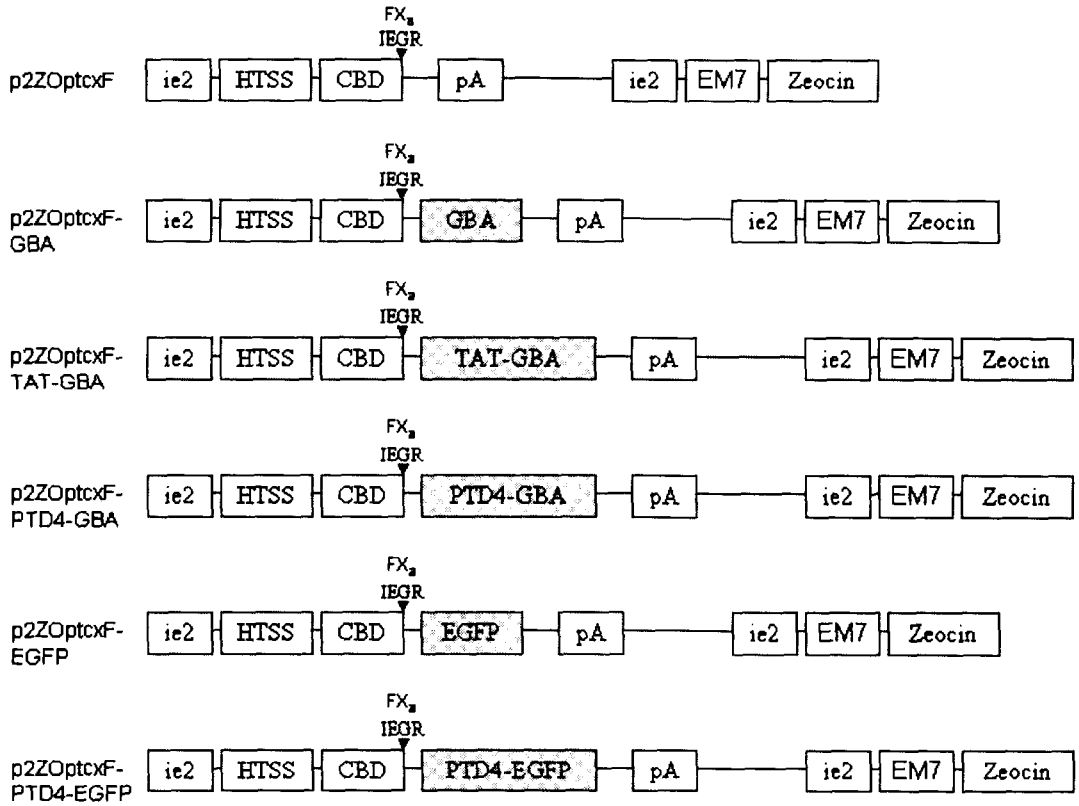

Figure 2.1. Acid β-glucosidase (GBA) and Enhanced Green Fluorescent Protein (EGFP) fusion vectors constructed for the expression of HIV-I TAT and PTD4 protein transduction domain fusion proteins. Expression for all constructs was initiated from the *Orgyia psuedotsugata ie2* promoter (ie2) for secretion using the human transferrin secretion signal (HTSS) present in the p2ZOptcxF vector backbone (donation from Dr. T. Pfeifer). The cellulose binding domain (CBD) affinity tag with its C-terminal Factor X_a cleavage site (FX_a-IEGR) and the *ie2* polyadenylation site (pA) are noted. The *ie2*-synthetic bacterial EM7 promoter (ie2/EM7) to drive the expression of the Zeocin™-resistance gene of *Streptoalloteichus hindustanus ble* (Zeocin) is also shown. Constructs are not drawn to scale.

PTD-4 sequence attached to the 5' end of GBA, denoted as p2ZOptcxF-PTD4-GBA.

To create the plasmid containing the 756 bp *egfp* insert, the *egfp* cDNA from pEGFP-N1 (Clontech, Palo Alto, CA) was PCR-amplified by primers E1 and E2, which contain *Eco*RI restriction sites. Creation of the desired p2ZOptcxF-EGFP plasmid was performed in the same manner as p2ZOptcxF-GBA.

The p2ZOptcxF-PTD4-EGFP plasmid was created in the same manner as the PTD4-GBA construct using a large forward primer (E3) that encodes an *Eco*RI cut site, the entire sequence of PTD-4 and the first 15 bp of the *egfp* cDNA. In conjunction with primer E2 and using pEGFP-N1 as template, a 787 bp fragment was produced for cloning into p2ZoptcxF.

2.2.2 Restriction digest of the p2ZOptcxF vector

To linearize the p2ZOptcxF vector and create sticky ends for cloning, 1 μg of vector was digested overnight with 20 units of *Eco*RI restriction enzyme (New England Biolabs, Beverly, MA) in 1X NEBuffer EcoRI (50 mM NaCl, 100 mM Tris-HCl, 10 mM $MgCl_2$, 0.025% Triton X-100 (v/v), pH 7.5) at 37°C. Concurrently the 5' phosphate groups of the exposed DNA ends were removed with 10 units of calf intestinal phosphatase (New England Biolabs, Beverly, MA). After digestion and dephosphorylation, the linearized vector was purified with the Qiaquick PCR purification kit (Qiagen, Mississauga, ON) following manufacturer's instructions.

2.2.3 Restriction digestion of insert DNA

DNA inserts encoding genes of interest were digested with *Eco*RI restriction enzyme to create sticky ends complementary to those of the digested and dephosphorylated p2ZoptcxF vector. In each case, 1 μg of PCR amplified DNA was digested with 20 units of *Eco*RI and 1X NEBuffer *Eco*RI in a final volume of 30 μl, at 37°C for 4 hours. Digested DNA was purified with the Qiaquick PCR purification kit according to the manufacturer's instructions.

2.2.4 Ligation of DNA inserts into the linearized p2ZOptcxF vector

Ligation of the vector and inserts was carried out in a ten minute reaction with 400 units of T4 DNA ligase (New England Biolabs, Beverly, MA) and 1X T4 DNA ligase buffer (50 mM Tris-HCl, pH 7.5, 10 mM $MgCl_2$, 10 mM dithiothreitol, 1 mM ATP, 25 μg/ml bovine serum albumin). A total of 100 μg of digested, dephosphorylated vector was used with a 1:1 ratio of pmole ends of insert, calculated with the following formula: (ng of vector x kb size of insert / kb size of vector) x (insert:vector molar ratio) = ng of insert. As a control, the same reaction was performed on vector without an insert, to determine the number of clones that result from re-ligation of the vector to itself.

2.3 Bacterial Transformation

2.3.1 Electroporation of E.coli with ligated vector and inserts

Purified, ligated plasmids were electroporated into Top10F' *E. coli* by combining 2 μl of the ligation reaction with 40 μl of electrocompetent *E. coli*, produced using the

protocol of Sambrook *et al.* (2001). Cells were pulsed in 0.1 cm gap cuvettes (BioRad Laboratories, Hercules, CA) at 1.5 kV on a GenePulser machine (BioRad Laboratories, Hercules, CA) with the setting of resistance 5. Directly following electroporation, 1 ml of SOC medium (2% tryptone (w/v), 0.5% yeast extract (w/v), 10 mM $NaCl_2$, 2.5 mM KCl, 10 mM $MgCl_2$-$6H_2O$, 10 mM $MgSO_4$-$7H_2O$) was added and the cells were incubated at 37°C for 1 hour, before being spread plated on low salt Luria Broth (LSLB)-Zeocin™ (25 μg/ml; Invitrogen Canada, Burlington, ON) plates for overnight incubation at 37°C.

2.3.2 Screening for true positives

Sixteen to twenty-four hours after electroporation, resulting Zeocin™-resistant colonies of *E. coli* were screened for the presence of plasmids by PCR. Briefly, colonies were picked with sterilized toothpicks and masterplated on LSLB-Zeocin™ (25 μg/ml) plates, while the remaining cells were swirled in 50 μl of ddH_2O, boiled for 5 min, and centrifuged at 14000 x g for 1 minute. Five (5) μl of the resulting supernatant were used as template in a screening PCR using one primer complementary to the vector and one within the insert of interest, so as to determine presence of plasmids as well as directionality of the insert DNA within the p2ZOptcxF vector. For all of the clones, the MCSF sense primer (5'- GGTTTCCAAGGTTCTCACACC –3') was used. The G2 anti-sense primer was used to identify positive p2ZOptcxF-GBA, p2ZOptcxF-TAT-GBA and p2ZOptcxF-PTD4-GBA clones. The E2 primer was used for p2ZOptcxF-EGFP and p2ZOptcxF-PTD4-EGFP clones (See Table 2.1 for anti-sense primer sequences). PCR conditions were as follows: 2.5 mM $MgCl_2$, 0.25 mM dNTPs, 1X UltraTherm PCR buffer, 0.6 μM forward and reverse primers, 0.5 units of UltraTherm polymerase

(Bio/Can Scientific, Mississauga, ON). Cycling was done as follows: 3 min 94°C hot start; 30 cycles of 1 min 94°C, 2 min 60°C, 2 min 72°C; and a final elongation at 72°C for 5 min. All resulting PCR products were visualized on 0.7% (w/v) agarose gels stained with 20 ng/ml ethidium bromide (Fisher Scientific, Fair Lawn, NJ), trans-illuminated with UV light and photographed using the EagleEye digital camera system (Stratagene, La Jolla, CA). Additional confirmation of true positives was done by linearization of the plasmids with *Xba*I (New England Biolabs, Beverly, MA) and determination of their size on a 0.7% (w/v) agarose gel stained with 20 ng/ml ethidium bromide. Digests were performed in 1X NEBuffer 2 (10 mM Tris-HCl,pH 7.9; 50 mM NaCl; 10 mM $MgCl_2$, 1 mM dithiothreitol) supplemented with 100 µg/ml bovine serum albumin with 20 units of *Xba*I. Gels were visualized via UV trans-illumination and the Eagle Eye digital camera system.

2.3.3 DNA sequencing

A minimum of four *E. coli* clones identified by PCR to contain plasmids with inserts incorporated in the correct orientation were purified using the Qiaprep Miniprep kit (Qiagen, Mississauga, ON) according to the manufacturer's instructions. Plasmids were sequenced on a CEQ 8000 automated sequencer (Beckman-Coulter, Fullerton, CA) using a dye-terminator dideoxy sequencing method (UVIC Centre for Biomedical Research DNA Sequencing Facility, Victoria, BC). DNA sequence trace data was analyzed using the SeqMan software (DNASTAR, Madison, WI) to determine clones that were mutation free and could be used for transfection into the insect expression system.

2.4 Insect Transfection

2.4.1 Lipofection of Sf9

Prior to transfection, *Sf9* cells were grown at 27°C to mid-log phase in Sf900II SFM medium (Invitrogen Canada, Burlington, ON). For stable transfections, 1 x 10^6 cells were seeded in a 6 well culture plate and allowed to attach overnight. Mutation-free plasmids were lipofected into *Sf9* insect cell culture using Cellfectin reagent (Invitrogen Canada, Burlington, ON) at a ratio of 10 µl reagent to 1 µg of plasmid DNA. Briefly, 10 µl of reagent were resuspended in 100 µl of Sf900II SFM media, and 1 µg of plasmid DNA was resuspended in a separate 100 µl of media. The resuspended DNA and reagent were mixed and allowed to incubate for 30 min followed by the addition of 800 µl of Sf900II SFM medium. Medium was removed from 70% confluent *Sf9* cells and replaced with the lipofection mixture. Cells were incubated at 27°C for 18 hours before medium was changed with fresh Sf900II SFM. Cells were grown to confluence, harvested and plated into T25 tissue culture flasks with 5ml of Sf900II SFM media and 0.5 mg/ml Zeocin™ to begin selection of stable integrants.

2.4.2 Zeocin resistance selection of stable polyclonal cultures

Multiple integration events can occur within the *Sf9* genomic DNA and can be selected by growing cells with increasing concentrations of antibiotic. Zeocin™ selection at 0.5 mg/ml was started 48 hours post-lipofection when the *Sf9* cells were scaled up to T25 culture flasks. Once cells reached confluence they were scaled to T75 culture flasks

and the Zeocin™ concentration was increased to 0.75 mg/ml. A further passage was done in T75 flasks with the Zeocin™ concentration being increased to 1.0 mg/ml.

2.4.3 Large scale Sf9 cultures

Polyclonal, 1.0 mg/ml Zeocin™-resistant cell lines were scaled-up to 60 ml shaker flasks to allow large-scale cell culture and protein production. Shaker flasks (250 ml) were seeded at 5 x 10^5 to 1 x 10^6 cells/ ml with 60 ml of Sf900II SFM medium and 1 mg/ml Zeocin™. Flasks were aerated by rotation at 125 rpm on a bench top shaker in a 27°C incubation room. Cultures were monitored by cell density and viability counts using a haemocytometer and 0.4% (w/v) trypan blue (Sigma Aldrich Canada, Oakville, ON) exclusion. Cultures were harvested when they reached 1.5 x 10^7 cells/ml and viability decreased below 80%. Cells were pelleted at 200 x g using a Sorvall SS34 rotor and RC 26 Plus ultracentrifuge (Kendro Laboratory Products, Ashville, NC). Medium and cell pellets were separated and stored at -20°C until needed.

2.5 DNA, RNA and Protein Analysis

2.5.1 Integration of Plasmid DNA into Sf9 Genomic DNA

Zeocin™-resistant *Sf9* cell cultures were assayed for the incorporation of plasmid DNA into the host genome by isolating the insect genomic DNA from 5 x 10^6 cells with a DNeasy Tissue Kit (Qiagen, Mississauga, ON). Purified genomic DNA (150 ng) was used as template for a PCR reaction to specifically amplify the integrated plasmid DNA. For each *Sf9* transfected cell line, primers were utilized that are complementary to the *ie2*

promoter upstream of the multiple cloning site (MCS) in the p2ZOptcxF vector (primer ie2F – 5'-CTATAAATACAGCCCGCA-3') and to the vector sequence downstream of the MCS (primer MCSR – 5'- CACGCGCTTGAAAGGAGTGT-3'). PCR reaction conditions were as follows: 2.5 mM $MgCl_2$, 0.25 mM dNTPs, 1X UltraTherm PCR buffer, 0.6 μM forward and reverse primers, 0.5 units of UltraTherm polymerase. Cycling was done as follows: 3 min 94°C hot start, 30 cycles of 1 min 94°C, 2 min 60°C, 2 min 72°C, and a final elongation at 72°C for 5 min. PCR products were run on 0.7% (w/v) agarose and visualized with 20 ng/ml ethidium bromide staining. Images were taken with UV trans-illumination and the Eagle Eye digital camera system.

2.5.2 RNA Isolation and RT-PCR

To confirm that integrated plasmid DNA was being transcribed by the *Sf*9 system, total RNA was isolated from 5 x 10^6 cells using the RNeasy Mini Kit (Qiagen. Missisauga, ON). The manufacture's spin protocol for isolation of total RNA from animal cells was followed with the addition of the optional RNase-Free DNase set (Qiagen, Missisauga, ON). To produce a cDNA library, reverse transcriptase PCR (RT-PCR) was performed on 1 μl of the RNA extraction with 0.5 μg oligo-$(dT)_{15}$ primer (Qiagen Operon, Mississauga, ON), 0.83 mM dNTPs. This solution was heated to 65°C for 5 minutes, followed by a brief chilling on ice. Invitrogen Superscript II First-Strand buffer (50 mM Tris-HCl, pH 8.3, 75 mM KCl, 3mM $MgCl_2$) and 0.01 M dithiothreitol were added and incubated at 42°C for two minutes, followed by the addition of 50 units of Superscript II Reverse Transcriptase (Invitrogen Canada, Burlington, ON). Fifty (50)

minutes of incubation at 42°C and heat inactivation at 70°C for 15 minutes completed the cDNA synthesis reaction. The First-Strand cDNA product was utilized in a PCR with primers specific to the genes of interest. In all cases, the HTSSF primer (5'-ACCCAAGCTTATGAGGCTCGCCGTG-3') was utilized. For clones containing the *gba* gene, the G2 anti-sense primer was used, and for the *egfp*-containing clones, the E2 primer was used (see Table 2.1 for anti-sense primer sequences). PCR products were run on 0.7% agarose (w/v), stained with 20 ng/ml ethidium bromide, and visualized by UV trans-illumination and the Eagle Eye digital camera system.

2.5.3 Western Blot Analysis of Protein Expression

Confirmation of protein expression was done via Western immunoblotting with anti-GBA, anti-EGFP and anti-CBD specific antibodies. In all cases, 5 x 10^6 cells were harvested from a 120 hour shaker culture and centrifuged at 200 x g to separate cells from the medium. The resulting medium was concentrated to 1-5 μg/μl total protein with 30,000 NMWL Nanosep centrifugal devices (Pall Corporation, East Hills, NY). The cell pellet was resuspended in lysis buffer (50 mM Tris, pH 7.8, 150 mM NaCl, 1% Triton X-100 (v/v) and 1 mM PMSF), vortexed for 2 minutes and centrifuged at 14,000 x g for 5 minutes. The resulting supernatant was used directly as the cytoplasmic fraction and the pellet was resuspended in 100 μl PBS and utilized as the membrane fraction. Total protein concentration was determined for both the concentrated medium and the cytoplasmic fractions using the BioRad Protein Assay (BioRad Laboratories, Hercules, CA) and a BSA standard curve (0-0.7 mg/ml; New England Biolabs, Beverly, MA). Ten

(10) μg of total protein were used for both the medium and cytoplasmic fractions, with a volume equal to that of the cytoplasmic fraction used for the membrane fraction.

For immunoblotting with the anti-EGFP antibody, a recombinant EGFP protein (Clontech, Palo Alto, CA) was used as a control. For anti-GBA Westerns, medium from a *Sf*9 culture known to express high levels of active, glycosylated GBA was used (designated 3-1B, donation from Dr. G. Sinclair, University of British Columbia, Vancouver, BC). Westerns for anti-CBD detection, employed a recombinant CBD_{Cex} protein (donation from Dr. R.A.J. Warren, University of British Columbia, Vancouver, BC) as a positive control. For each sample, 7 μl of 3X SDS loading buffer (Invitrogen Canada, Burlington, ON) were added to the samples and brought up to 21 μl with ddH_2O. Samples were boiled 5 minutes, centrifuged at 14,000 x g for 1 minute and loaded along with controls and a Broad Range Protein standard (New England Biolabs, Beverly, MA), in a 10% (v/v) tris-glycine SDS-PAGE gel prior to electrophoresis for one hour with the Emperor Penguin™ Dual Gel Vertical Electrophoresis System (Owl Separation Systems, Portsmouth, NH).

Resulting protein bands were electroblotted from SDS-PAGE gels onto Hybond-P PVDF membrane (Amersham, Piscataway, NJ) overnight at 10V in 10% (v/v) methanol transfer buffer (25 mM Tris-HCl, 0.2 M glycine) using a Mini-protean II Electroblot Apparatus (BioRad, Hercules, CA). All following steps were performed at room temperature with gentle agitation. PVDF membranes were blocked for 1 hour in TTBS (20 mM Tris-HCl, pH 7.5, 0.05% Tween-20 (v/v), 500 mM sodium chloride) with 7.5% (w/v) dry skim milk powder. A 1:500 dilution of anti-GBA antibody (donation of Dr. E. Beutler, Scripps Research Institute, La Jolla, CA), 1:5000 dilution of anti-EGFP antibody

(Clontech, Palo Alto, CA) or 1:500 anti-CBD antibody (Novagen-EMD Biosciences, San Diego, CA) was added to the blocking solution and incubated for one hour. Membranes were washed 3 times with TTBS, then incubated for 1 hour with a 1:5000 dilution of rabbit anti-mouse horseradish peroxidase conjugated antibody (Sigma-Aldrich Canada, Oakville, ON) for anti-GBA and anti-EGFP blots, or a 1:50,000 dilution of goat anti-rabbit horseradish peroxidase conjugated antibody (Stressgen, Victoria, BC) for anti-CBD blots. Membranes were again washed 3 times in TTBS, incubated with ECL+ chemiluminescent reagent (Amersham, Piscataway, NJ) for 5 minutes, and visualized via autoradiography with Kodak BioMax MR film (Eastman Kodak, Rochester, NY).

2.5.4 Epi-fluorescence Microscopy of EGFP Clones

Sf9 cells expressing the EGFP and PTD4-EGFP proteins were visualized with epi-fluorescence microscopy using the 485 nm excitation filter and 528 nm emission filter set on a Zeiss Universal microscope (Carl Zeiss Canada, North York, ON). Cells were removed from 1 X 10^7 cells/ml suspension cultures and placed on glass slides with coverslips to allow visualization of living cells. Photographs were taken within 2 minutes of focusing on the field of view to minimize the effects of photobleaching, using a FinePix 990 digital camera (Fuji Photo Film, Tokyo, Japan).

2.5.5 Fluorescence Quantification of EGFP Clones

The amount of EGFP or PTD4-EGFP protein produced by *Sf9* cells was quantified using the Synergy HT-I microtitre plate reader and KC4 software (Biotek,

Winooski, VT). An EGFP protein standard curve was produced using purified recombinant EGFP protein (Clontech, Palo Alto, CA) within the linear range of 0 to 800 ng. Protein was resuspended in 100 µl of TBS, pH 7.5, with TBS being used as a blank. Relative fluorescence unit (RFU) readings were taken with the 485/20 nm excitation filter and 528/20 nm emission filter at a sensitivity of 69. Standard curves were produced using Excel software (Microsoft Canada Co, Mississauga, ON) and unknown EGFP protein concentrations were calculated with the following equation: RFU = 93.2 (ng of fluorescent protein). One hundred (100) µl of media from EGFP and PTD4-EGFP cultures grown to 1 x 10^7 cells/ml were measured for relative fluorescent units using the above settings. Medium from *Sf*9 wildtype cells grown to the same density was used as a blank.

2.5.6 GBA Enzyme Activity Assay

Acid β-glucosidase (GBA) activity in the culture medium was assayed using the artificial substrate 4-methyl-umbelliferyl-β-D-glucopyranoside (4MUGP) (Sigma-Aldrich Canada, Oakville, ON). Culture media from the *Sf*9 cultures were utilized directly or the soluble proteins were concentrated by Nanosep 30,000 NMWL centrifugal concentrators prior to activity assay.

GBA activity assay with 4MUGP was performed following the protocol of Choy (1984). Briefly, 4MUGP (3.5 mM), citrate buffer (0.03 M, pH 5.5), sodium taurocholate (0.1% (w/v)) and the GBA containing sample were mixed and incubated at 37°C for 30 minutes. The reaction was stopped by adding an excess of 0.2 M glycine buffer (pH 10.5) and fluorescence assayed using a Synergy HT microtitre plate reader and the KC4 data

capture software. Raw fluorescence readings were compared to a 4-methyl-umbelliferone (4MU; Sigma Aldrich Canada, Oakville, ON) standard curve to calculate moles of 4MU released and the relative and/or specific activity of the sample. All protein concentrations were calculated using the BioRad Protein Reagent (BioRad, Hercules, CA) as adapted from Bradford (1976).

2.6 Purification of heterologous proteins

2.6.1 Concentration of Secreted Proteins

Due to the low concentration of recombinant protein identified on the Western blots, medium containing secreted protein of interest was concentrated to allow better binding to cellulose for affinity purification. Briefly, 200 ml of medium were concentrated to less than 10 ml with an Amicon stirred cell apparatus (Millipore, Billerica, MA) under 50 psi pressure. For EGFP-containing proteins a 10,000 NMWL polyethersulfone membrane (Millipore, Billerica, MA) was used. Concentrated medium was stored at 4°C until needed.

2.6.2 Cellulose binding of CBD-tagged proteins

Affinity purification of proteins of interest was accomplished by binding of the CBD fusion proteins onto Sigmacell™ cellulose (Sigma-Aldrich Canada, Oakville, ON). Initially, 5 mg of Sigmacell™ were added to 10 ml of unmodified culture medium and incubated at 4°C overnight with vigorous shaking, following the protocol of Assouline *et al.* (1993). Due to poor specificity of binding, conditions were altered. Briefly, the pH of 10 ml of culture media containing the secreted fusion proteins was adjusted to 8.5 with

1M NaOH, and was brought to a final concentration of 0.1% TRITON X-100 (v/v). Protein precipitation followed on ice for 20 minutes. Precipitate was collected by centrifugation at 5000 x g for 5 minutes and the supernatant was used for binding to 5 mg of washed Sigmacell™ (washed 10X with ddH_2O, 2X with TBS, pH7.4). Binding proceeded overnight at 4°C with vigorous shaking in order to keep the cellulose in suspension.

2.6.3 Silver stain of cellulose-purified proteins

Cellulose-bound proteins were eluted and visualized on tris-glycine, sodium dodecyl-sulfate (SDS) polyacrylamide gel electrophoresis (PAGE) as described (Spector *et al.*, 1998). Bound protein was eluted from the cellulose using 3X SDS loading buffer, boiled for 5 minutes. Samples were electrophoresed on a 4% (v/v) stacking and 10% (v/v) resolving SDS-PAGE gel, run at 20 mA for approximately one hour in an Emperor Penguin™ Dual Gel Vertical Electrophoresis System.

Proteins were visualized on SDS-PAGE gels using silver stain as follows. Gels were microwaved at maximum power for 90 seconds in fixative (50% (v/v) methanol, 12% (v/v) acetic acid, 0.1% (v/v) formaldehyde) followed by a 90s microwave in 50% (v/v) ethanol. The gels were then pretreated in 0.02% (w/v) sodium thiosulfate-pentahydrate for 90s in the microwave, washed in ddH_2O for 90s at room temperature and stained in 2 mg/ml silver nitrate in 0.075% (v/v) formaldehyde by microwaving twice for 40s. Bands were resolved in developer (60 mg/ml sodium carbonate, 0.05% (v/v) formaldehyde, 0.002% (w/v) sodium thiosulfate pentahydrate and the reaction stopped in 50% (v/v) methanol following a 90s water wash. Gels were dried in 4% (v/v) glycerol

between sheets of cellophane with an Easy Breeze™ air gel-drying apparatus (Amersham, Piscataway, NJ).

2.6.4 Western blotting of cellulose-purified proteins

Detection of the proteins of interest that bound onto cellulose, was performed by Western immunoblotting. Proteins were removed from cellulose with 1X SDS buffer and boiling for 5 minutes. Denatured proteins were run on SDS-PAGE as described (Spector *et al.*, 1998), using an Emperor Penguin™ Dual Gel Vertical Electrophoresis System. Protein bands were transfer from the SDS-PAGE to PVDF overnight at 10V with a Mini-protean II Electroblot Apparatus. Non-specific binding to the PVDF membrane was blocked by washing the membrane in 7.5% (w/v) skim milk powder in TTBS for one hour. Primary antibody (1:500 anti-GBA, 1:5000 anti-EGFP, or 1:500 anti-CBD) was then added for one hour, followed by three 10 minute washes in TTBS. Horseradish peroxidase (HRP) conjugated secondary antibody, specific to the primary antibody (1:5000 rabbit anti-mouse IgG-HRP for GBA and EGFP primary antibodies, and 1:50,000 goat anti-rabbit IgG-HRP for CBD primary) was added for one hour, followed by three 10 minute washes in TTBS. Chemiluminescent detection of HRP was performed with the ECL+ Western Blotting detection kit and autoluminography using BioMax MR film.

2.6.5 Factor X_a cleavage of cellulose-bound proteins

Proteins of interest were purified from other natively produced *Sf9* proteins using cellulose binding domain affinity purification. Once bound overnight, cellulose pellets

were washed twice with TBS, pH 7.5 containing 0.1% (v/v) TRITON X-100, followed by two washes in TBS, pH 7.5. The washed pellet was resuspended in 200 µl of 70% (v/v) ethylene glycol and incubated at 4°C overnight with agitation. Two additional ten minute incubations with 100 µl of 70 % (v/v) ethylene glycol were performed the following morning, at room temperature. Eluted protein was then dialyzed into TBS, pH 7.5 and concentrated using a Nanosep 30,000 NMWL centrifugal concentrator. Factor X_a (EMD Biosciences, San Diego, CA) was added to the pure protein (0.02 units/µg of protein) and cleavage proceeded overnight at 25°C. Cleaved proteins were harvested from the supernatant and contaminating Factor X_a proteins were removed with the Novagen Factor X_a Cleavage Capture kit (EMD Biosciences, San Diego, CA) following the manufacturer's instructions. Contaminating cellulose binding domains were removed by overnight binding to 2 mg of Sigmacell™. The purified protein was concentrated using Nanosep 30,000 NMWL centrifugal concentrating devices as per manufacturer's protocol.

2.7 Transduction Study of PTD4-EGFP and EGFP Proteins

2.7.1 Transduction Study of PTD4-EGFP and EGFP Proteins with Sf9 cells

Following the work of Barka *et al.* (2004), transduction of the PTD4-EGFP was attempted on wildtype cells, of the type used for the expression of the fusion protein. The medium containing the PTD4-EGFP protein was concentrated with an Ultrafree 4 centrifugal concentrator (Millipore, Billerica, MA). Concentrated medium was used to resuspend a 5 x 10^6 cell pellet of wildtype *Sf*9 cells. This was done in triplicate to allow monitoring at 10, 30 and 60 minutes. As controls, concentrated medium from EGFP secreting cells and wildtype *Sf*9 cells were also tested on pellets of *Sf*9 cells. After the

appropriate incubation, 10 μl of resuspended cells were mixed 1:1 with 0.4% (w/v) trypan blue and mounted on glass slides with coverslips. Cells were visualized with the 485 nm excitation and 528 nm emission filter set on a Zeiss Universal microscope. Photographs were taken with a FinePix 990 digital camera.

3 Results

3.1 Plasmid Construction and Bacterial Transformation

PCR amplification successfully produced the DNA inserts for GBA, TAT-GBA, PTD4-GBA, EGFP and PTD4-EGFP. Figure 3.1 shows bands within a 0.7% (w/v) agarose gel for each of the inserts of interest. The expected DNA inserts sizes are: 1558 base pairs (bp) for GBA, 1595 bp for TAT-GBA and PTD4-GBA, 756 bp for EGFP, and 787 bp for PTD4-EGFP.

Using the DNA inserts the following plasmids were successfully constructed and used to transform Top10F' cells: p2ZOptcxF-GBA, p2ZOPtcxF-TAT-GBA, p2ZOptcxF-PTD4-GBA, p2ZOPtcxF-EGFP, p2ZOptcxF-PTD4-EGFP, p2ZOptcxF-TAT and p2ZOptcxF-PTD4. Figure 3.2 shows bands within a 0.7% (w/v) agarose gel corresponding to *Xba*I linearized plasmids containing each of the inserts of interest. Expected plasmid sizes are as follows: 3186 bp for p2ZOptcxF, 4732 bp for p2ZOptcxF-GBA, 4771 bp for p2ZOptcxF-TAT-GBA and p2ZOptcxF-PTD4-GBA, 3914 bp for p2ZOPtcxF-EGFP, and 3952 bp for p2ZOptcxF-PTD4-EGFP. Sequencing results confirmed the absence of mutations in all vectors.

3.2 Sf9 Transfection and Genomic DNA Integration of p2ZoptcxF Plasmids

*Sf*9 cells were successfully transfected with P2ZOptcxF-GBA, p2ZoptcxF-TAT-GBA, p2ZoptcxF-PTD4-GBA, p2ZoptcxF-EGFP, and p2ZoptcxF-PTD4-EGFP, as indicated by the cultures' resistance to the antibiotic Zeocin™.

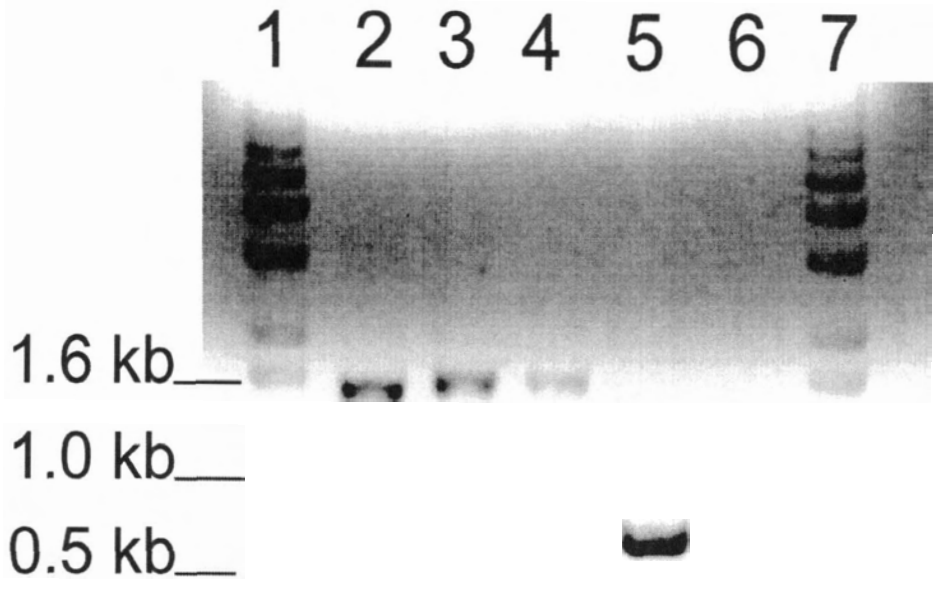

Figure 3.1. Agarose gel of DNA inserts for GBA (Lane 2), TAT-GBA (Lane 3), PTD4-GBA (Lane 4), EGFP (Lane 5) and PTD4-EGFP (Lane 6) to be cloned into the p2ZOptcxF vector. A 1 kb DNA standard (Invitrogen Canada, Burlington, ON) was run (Lanes 1 and 7) to determine the size of the DNA bands. DNA was stained with ethidium bromide.

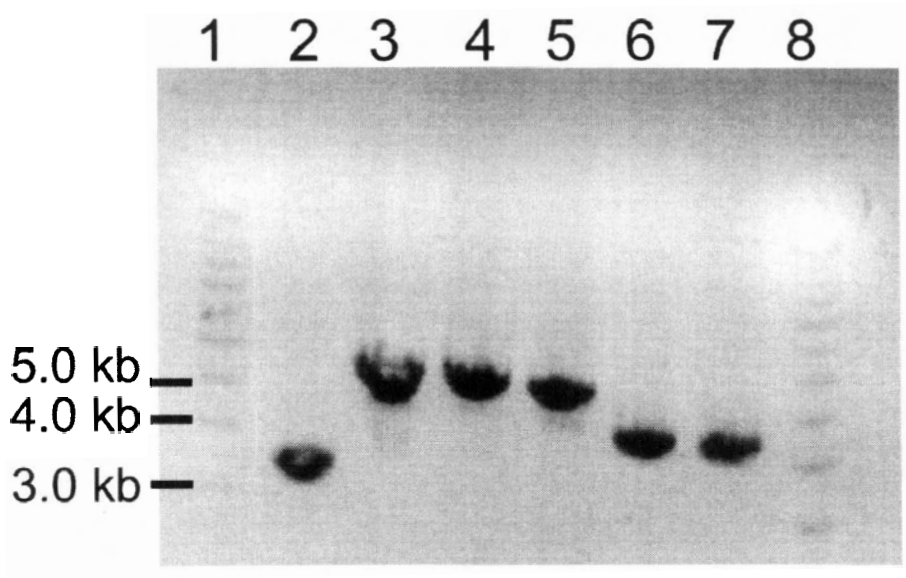

Figure 3.2. Agarose gel of *Xba*I linearized plasmids constructed with p2ZOptcxF vector backbone. From left to right (Lanes 1-6): p2ZOptcxF, p2ZOptcxF-GBA, p2ZOptcxF-TAT-GBA, p2ZOptcxF-PTD4-GBA, p2ZOptcxF-EGFP, p2ZOptcxF-PTD4-EGFP. A 1 kilobase DNA standard (Invitrogen Canada, Burlington, ON) is present in Lanes 1 and 8 to allow size determination of the linearized plasmids. DNA was stained with ethidium bromide.

Genomic DNA extracted from stably transfected *Sf*9 cells was used as template for PCR reactions to amplify the specific genes of interest that were contained within the p2ZoptcxF constructs. With all constructs, the gene of interest could be amplified from *Sf*9 cell genomic DNA, demonstrating that the plasmid DNA had been successfully integrated into the host cell genome. Negative controls showed no amplification. Figure 3.3 illustrates positive genomic DNA PCR screening results. Bands in the 0.7% (w/v) agarose gel correspond to appropriate insert sizes for each vector. Expected band sizes are as follows: 2224 bp for p2ZOPtcxF-GBA, 2263 bp for p2ZOptcxF-TAT-GBA and p2ZOptcxF-PTD4-GBA, 1406 bp for p2ZOPtcxF-EGFP, 1445 bp for p2ZOptcxF-PTD4-EGFP and 678 bp for p2ZOptcxF vector without an insert.

The intensity of band staining may also indicate the number of insert copies integrated into the host genomic DNA due to the use of the same mass (150 ng) of genomic DNA used as template for the PCR reactions. For the EGFP containing clones the p2ZOPtcxF-EGFP (Figure 3.3, Lane 3) clone showed a band with approximately twice the intensity of the p2ZoptcxF-PTD4-EGFP (Lane 2) clone, which may indicate a greater copy number for the former clone. GBA containing clones also demonstrated variability in band intensity with the band from the p2ZoptcxF-PTD4-GBA (Lane 6) clone being much brighter than that of the p2ZoptcxF-GBA (Lane 4) and p2ZOPtcxF-TAT-GBA (Lane 5) clones.

3.3 Detection of mRNA from p2ZoptcxF Constructs

Once the presence of the genes of interest within the insect cell genomic DNA was confirmed, the corresponding mRNAs were sought to demonstrate that the genes

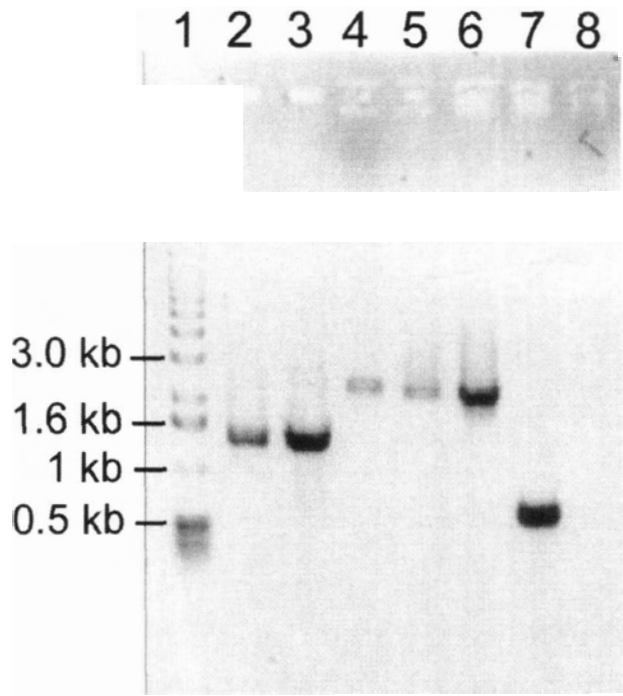

Figure 3.3. Polymerase chain reaction amplification of *Sf9* genomic DNA with gene-specific primers to confirm integration of the p2ZOptcxF constructs into the insect genome. All clones were PCR amplified using primers ie2F, complementary to the ie2 promoter and MCSR, complementary to the p2ZOptcxF vector, 100 bp downstream of the multiple cloning site. An expected band of 1445 bp is present (Lane 2) representing the p2ZOptcxF-PTD4-EGFP integrant. An expected band of 1406 bp is present for the p2ZOptcxF-EGFP clone (Lane 3). Integration of all three GBA clones; p2ZOptcxF-GBA (lane 4), p2ZOptcxF-TAT-GBA (Lane 5) and p2ZOptcxF-PTD4-GBA (Lane 6) are visible, with bands of 2224, 2263, and 2263 bp respectively. The vector-only control, p2ZOptcxF, shows a band of 678 bp, indicating integration of the vector without an insert in the multiple cloning site. As a negative control, mocked transfected *Sf9* cells, show no amplification (Lane 8). A 1 kb DNA standard ladder (Invitrogen Canada, Burlington, ON) was included for reference (Lane1). DNA in the agarose gel was stained with ethidium bromide.

were transcribed. In the case of each p2ZoptcxF construct, the presence of mRNAs was detected by RT-PCR with gene-specific primers. Figure 3.4 shows the expected band sizes: 1994 bp for p2ZOPtcxF-GBA, 2033 bp for p2ZOptcxF-TAT-GBA and p2ZOptcxF-PTD4-GBA, 1187 bp for p2ZOPtcxF-EGFP, and 1226 bp for p2ZOptcxF-PTD4-EGFP. Negative controls showed no amplification. In addition, all cultures showed amplification of the housekeeping gene for glyceraldehyde-3-phosphate dehydrogenase (GAPDH) mRNA as a control.

3.4 Sf9 Heterologous Protein Expression and Western Blot Protein Analysis

Due to the presence of the human transferrin secretion signal within the p2ZOptcxF vector, all of the heterologous proteins were expected to be secreted into the medium. As EGFP is a cytoplasmic protein and GBA is membrane-associated, the cytoplasmic and membrane fractions of transfected *Sf*9 cells were assayed, in addition to the medium, to determine the localization of the heterologous proteins of interest.

Protein within the medium was detected to be reactive with the anti-GBA antibody for the p2ZOptcxF-GBA, p2ZOptcxF-TAT-GBA and P2ZOptcxF-PTD4-GBA transfected *Sf*9 cultures (Figure 3.5). Apparent molecular masses of the secreted anti-GBA proteins were 65 kiloDaltons (kDa) for p2ZoptcxF-GBA, and 70 kDa for p2ZoptcxF-TAT-GBA and p2ZoptcxF-PTD4-GBA transfected cells. The cellulose binding domain (CBD)-tagged GBA, TAT-GBA and PTD4-GBA proteins ran slightly higher than the glycosylated, untagged 3-1B GBA control protein, but the expected mass of these proteins was 79 kDa for GBA and 81 kDA for TAT-GBA and PTD4-GBA in their tagged and glycosylated forms. The cytoplasmic and membrane fractions showed no

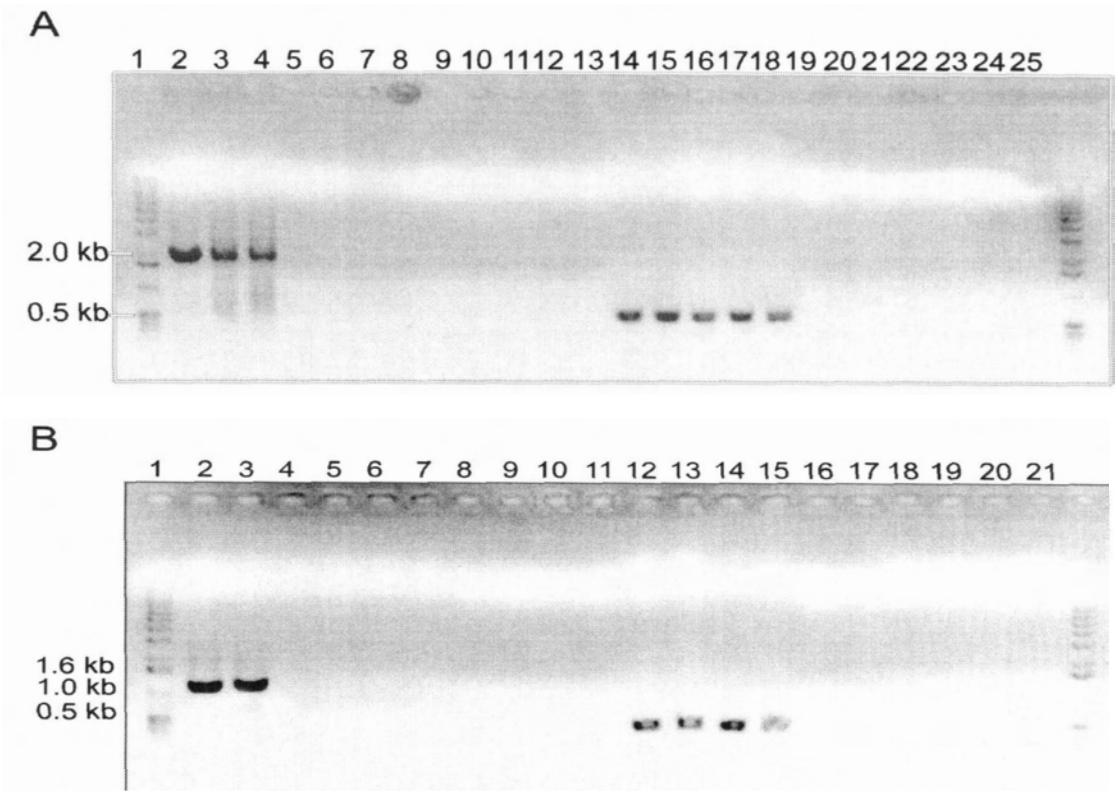

Figure 3.4. RT-PCR of mRNA extracted from transfected *Sf9* cells to determine if integrated genes were transcribed. First strand cDNA synthesis was used as template for the subsequent gene-specific primer PCR. A 1 kb DNA standard ladder (Invitrogen Canada, Burlington, ON) was included for reference in each gel (Lane 1). **(A)** Amplification of the GBA-containing mRNAs was performed with primers HTSSF and G2. An expected band of 1994 bp is present for p2ZOptcxF-GBA (Lane 2), 2033 bp for p2ZOptcxF-TAT-GBA (Lane 3) and p2ZOptcxF-PTD4-GBA (Lane 4). No amplification is seen for p2ZoptcxF vector only control (Lane 5), *Sf9* cells only control (Lane 6), no template first strand synthesis control (Lane 7), and no template control (Lane 8). In order to ensure that the PCR products were not due to DNA contamination of the extracted RNA, UltraTherm polymerase PCR was conducted on the RNA of p2ZOptcxF-GBA (Lane 9), p2ZOptcxF-TAT-GBA (Lane 10), p2ZOptcxF-PTD4-GBA (Lane 11), p2ZOptcxF vector only (Lane 12), and *Sf9* cells only (Lane 13). As a control the GAPDH mRNA was also amplified from the cDNA first strand synthesis reaction, using primers

GAPDHF and GAPDHR. Amplification of a 0.5 kb band is seen for p2ZOptcxF-GBA (Lane 14), p2ZOptcxF-TAT-GBA (Lane 15), p2ZOptcxF-PTD4-GBA (Lane 16), p2ZOptcxF vector only (Lane 17), and *Sf9* cells only (Lane 18). The no template first strand synthesis control (Lane 19) and no template control (Lane 20) show no amplification as expected. The RNA sample was again used as template for an UltraTherm polymerase PCR reaction using the primers GAPDHF and GAPDHR. Lack of amplification for p2ZOptcxF-GBA (Lane 19), p2ZOptcxF-TAT-GBA (Lane 20), p2ZOptcxF-PTD4-GBA (Lane 21), p2ZOptcxF (Lane 22) and *Sf9* cells only (Lane 23) confirm that no DNA contamination was present in the RNA samples. **(B)** Amplification of the EGFP-containing mRNAs was performed with primers HTSSF and E2. An expected band of 1187 bp is present for p2ZOptcxF-EGFP (Lane 2) and 1226 bp for p2ZOptcxF-PTD4-EGFP (Lane 3). No amplification is seen for p2ZOptcxF vector only control (Lane 4), *Sf9* cells only control (Lane 5), no template first strand synthesis control (Lane 6), and no template control (Lane 7). In order to ensure that the PCR products were not due to DNA contamination of the extracted RNA, UltraTherm polymerase PCR was conducted on the RNA of p2ZOptcxF-EGFP (Lane 8), p2ZOptcxF-PTD4-EGFP (Lane 9), p2ZOptcxF vector only (Lane 10), and *Sf9* cells only (Lane 11). As a control the GAPDH mRNA was also amplified from the cDNA first strand synthesis reaction, using primers GAPDHF and GAPDHR. Amplification of the 0.5 kb band is seen for p2ZOptcxF-EGFP (Lane 12), p2ZOptcxF-PTD4-EGFP (Lane 13), p2ZOptcxF vector only (Lane 14), and *Sf9* cells only (Lane 15). The no template first strand synthesis control (Lane 16) and no template control (Lane 17) show no amplification as expected. The RNA sample was again used as template for an UltraTherm PCR reaction using the primers GAPDHF and GAPDHR. Lack of amplification for p2ZOptcxF-EGFP (Lane 18), p2ZOptcxF-PTD4-EGFP (Lane 19), p2ZOptcxF (Lane 20) and *Sf9* cells only (Lane 21) confirm that no DNA contamination was present in the RNA samples.

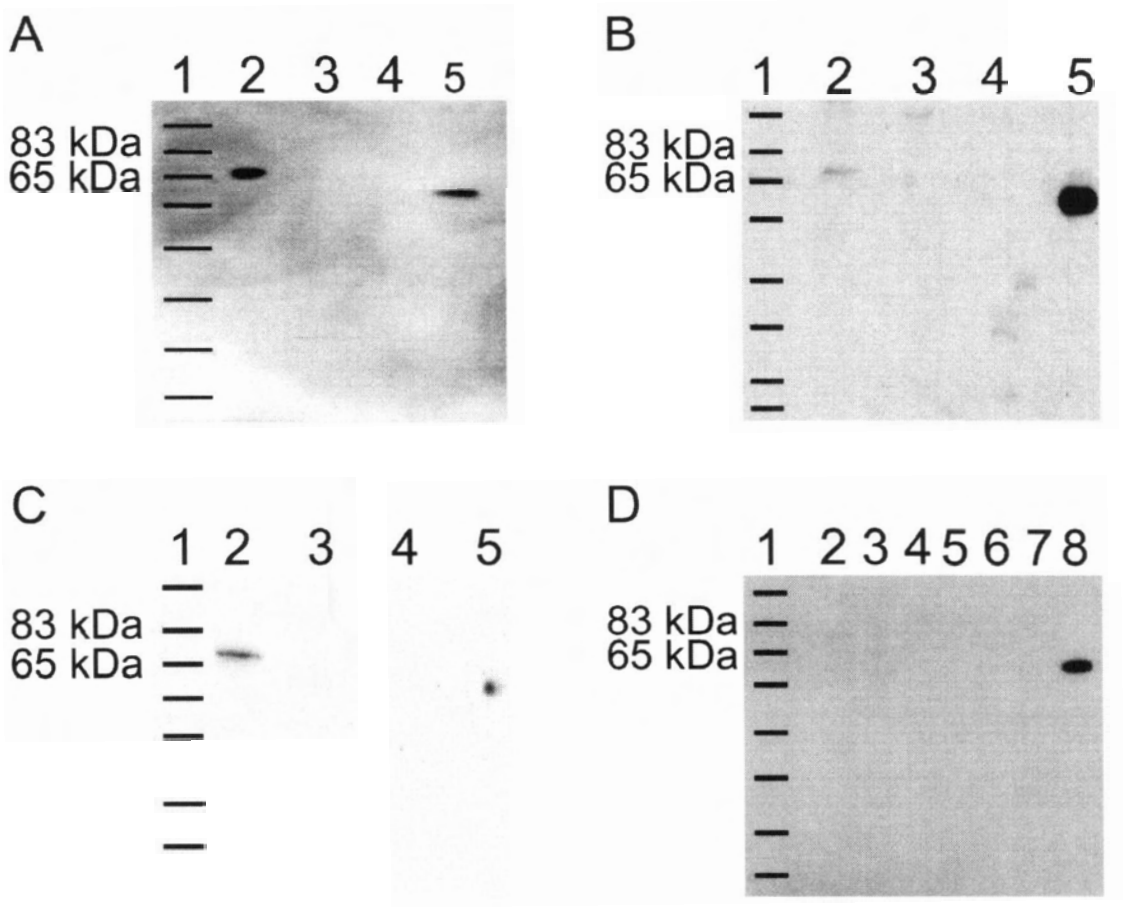

Figure 3.5. Western immunoblot of media, cytoplasmic and membrane fractions of p2ZOptcxF-GBA, p2ZOptcxF-TAT-GBA and p2ZOptcxF-PTD4-GBA transfected *Sf*9 cells, using a human acid β-glucosidase specific monoclonal antibody (AA16B3). In all cases, a control acid β-glucosidase protein (3-1B) was run as a positive control (Lane 5 for blots A-C and Lane 8 for blot D) and Broad Range Protein Standards (New England Biolabs, Beverly, MA) were used as a molecular mass reference (Lane 1) **(A)** Blot of p2ZOptcxF-GBA transfected cells medium (Lane 2), cytoplasmic fraction (Lane 3), and membrane fraction (Lane 4). **(B)** Blot of p2ZOptcxF-TAT-GBA transfected cells medium (Lane 2), cytoplasmic fraction (Lane 3), and membrane fraction (Lane 4). **(C)** Blot of p2ZOptcxF-PTD4-GBA transfected cells medium (Lane 2), cytoplasmic fraction (Lane 3), and membrane fraction (Lane 4). **(D)** Blot of p2ZOptcxF vector only transfected cells medium (Lane 2), cytoplasmic fraction (Lane 3), and membrane fraction (Lane 4), and wildtype *Sf*9 cells media (Lane 5), cytoplasmic fraction (Lane 6) and membrane fraction (Lane 7).

reactivity with the anti-GBA antibody. Control *Sf*9 cells and p2ZOPtcxF vector-only transfected cells showed no anti-GBA reactivity.

The medium, cytoplasmic and membrane fractions of p2ZOptcxF-GBA, p2ZOPtcxF-TAT-GBA and p2ZOptcxF-PTD4-GBA transfected cells were also immunoblotted with an anti-CBD antibody (Figure 3.6). No protein could be detected for the p2ZOptcxF-GBA transfected cells (data not shown). Protein within the medium was detected for both p2ZOPtcxF-TAT-GBA and p2ZOPtcxF-PTD4-GBA transfected cells. Apparent molecular masses are 70 kDA for the TAT-GBA and PTD4-GBA proteins, which is consistent with the masses determined from the anti-GBA antibody Western blots. No anti-CBD cross-reactive protein was detected for the wildtype *Sf*9 and p2ZOptcxF vector-only transfected cells.

Protein detection with the anti-EGFP antibody was achieved with the p2ZOptcxF-EGFP and p2ZOptcxF-EGFP transfected *Sf*9 cultures within the culture media (Figure 3.7). The secreted proteins that reacted with the anti-EGFP antibody had apparent molecular masses of 41 and 25 kDa for p2ZoptcxF-EGFP and 43, 27 and 19 kDa for p2ZoptcxF-PTD4-EGFP transfected cells. The multiple anti-EGFP cross-reactive bands are of the correct masses for a CBD-tagged EGFP or PTD4-EGFP protein (41 and 43 kDa, respectively) and an EGFP or PTD4-EGFP protein with the CBD tag cleaved off (25 and 27 kDa, respectively). The additional 19 kDa band from the p2ZOptcxF-PTD4-EGFP transfected cells may be a proteolytic cleavage product of the larger two protein species. Of all the transfected cultures, only the p2ZOptcxF-EGFP cells showed cross-reactive proteins within the cytoplasmic and membrane fractions (Figure 3.7, Lanes 3 and 4), but these proteins were of a smaller size than that expected for the CBD-tagged

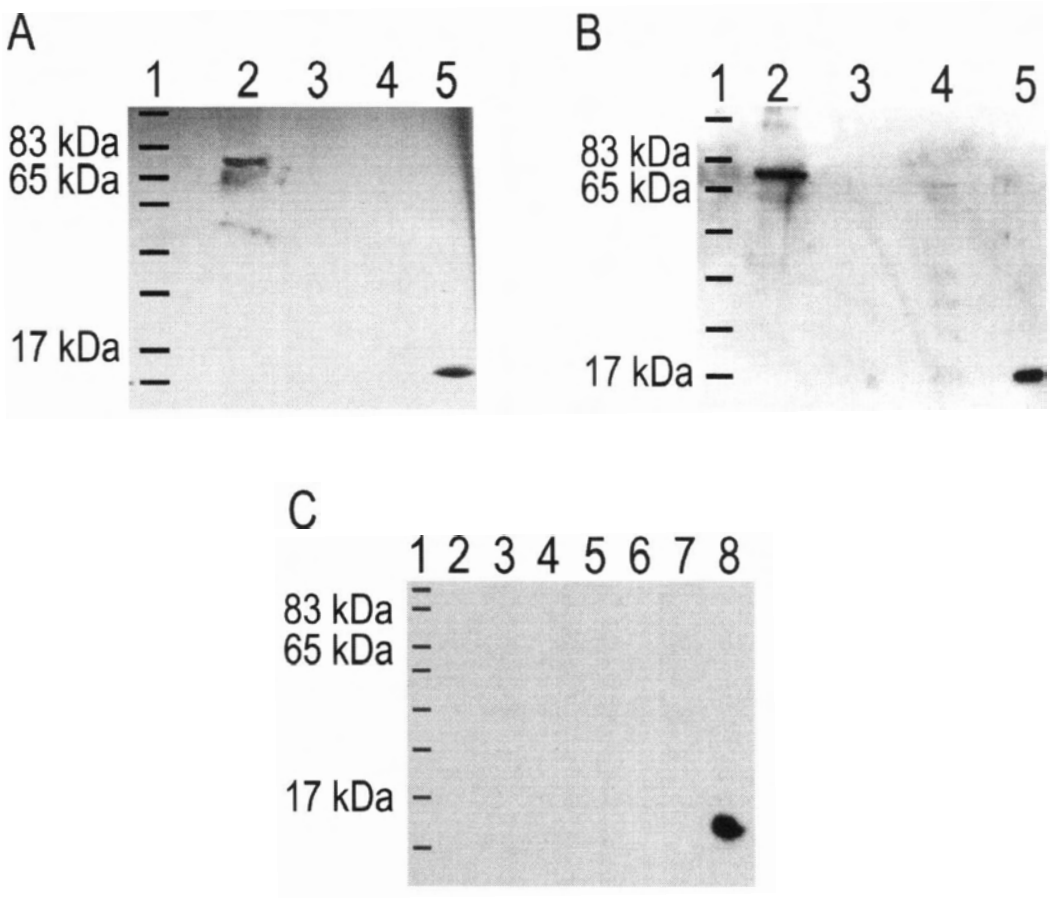

Figure 3.6. Western immunoblot of medium, cytoplasmic and membrane fractions of p2ZOptcxF-TAT-GBA, and p2ZOptcxF-PTD4-GBA transfected *Sf*9 cells, using a *Cex* cellulose binding domain specific monoclonal antibody. In all cases, a control *Cex* cellulose binding domain protein (generously provided by RAJ Warren, UBC, Vancouver, BC) was run as a positive control (Panels A and B: Lane5 and Panel C: Lane 8) and Broad Range Protein Standards (NEB) were used as a molecular mass reference (Lane 1) **(A)** Blot of p2ZOptcxF-TAT-GBA transfected cells medium (Lane 2), cytoplasmic fraction (Lane 3), and membrane fraction (Lane 4). **(B)** Blot of p2ZOptcxF-PTD4-GBA transfected cells medium (Lane 2), cytoplasmic fraction (Lane 3), and membrane fraction (Lane 4). **(C)** Blot of p2ZOptcxF vector only transfected cells medium (Lane 2), cytoplasmic fraction (Lane 3), and membrane fraction (Lane 4), and wildtype *Sf*9 cells medium (Lane 5), cytoplasmic fraction (Lane 6), and membrane fraction (Lane 7). The anti-CBD antibody detected no bands on the p2ZOptcxF-GBA-transfected cells Western blot (data not shown).

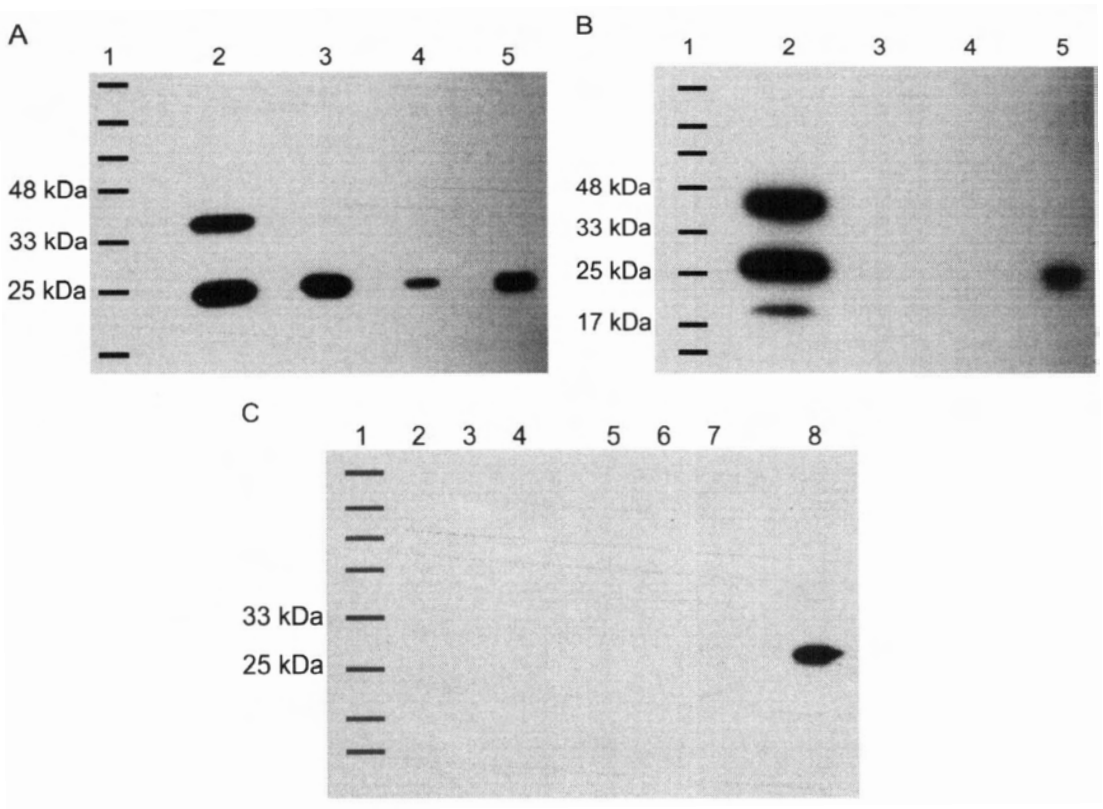

Figure 3.7. Western immunoblot of medium (Lane 2), cytoplasmic (Lane 3) and membrane (Lane 4) fractions of **(A)** p2ZOptcxF-EGFP and **(B)** p2ZOptcxF-PTD4-EGFP transfected *Sf*9 cells using EGFP specific monoclonal antibody (Clonetech, Palo Alto, CA). rEGFP protein (Clontech, Palo Alto, CA) was used as a positive control (Lane 6). As a negative control, **(C)** p2ZOptcxF vector-only transfected (Lanes 2-4) and wildtype *Sf*9 (Lanes 5-7) cells were prepared in the same manner. rEGFP protein (Clontech, Palo Alto, CA) was used as a positive control (Lane 8). On all blots, Broad Range Protein Standards (New England Biolabs, Beverley, MA) were included as a reference (Lane 1).

EGFP. The smaller anti-EGFP cross-reactive proteins were of the same mass (27 kDa) as the recombinant EGFP control protein and are likely the EGFP protein with the CBD removed.

3.5 Fluorescence Microscopy of EGFP and PTD4-EGFP Sf9 clones

Suspension cultures of stable integrants of the p2ZOptcxF-EGFP and p2ZOptcxF-PTD4-EGFP clones were grown to 1 x 10^7 cells/ ml and visualized with 450/585 nm filters on an epi-fluorescence microscope (Figure 3.8). EGFP cultures show cells with green fluorescence, whereas the PTD4-EGFP cultures did not show any fluorescent cells. The p2ZOptcxF vector-only transfected and wildtype *Sf*9 cells did not show any green fluorescence as expected. When analyzed in conjunction with the anti-EGFP Western immunoblot (Figure 3.7), it can be determined that although both the p2ZOptcxF- EGFP and p2ZOptcxF-PTD4-EGFP constructs have a human transferrin secretion signal, not all of the EGFP protein is secreted into the medium. With the addition of the PTD4 the PTD4-EGFP protein is fully secreted, though fluorescence could not be visually detected as the medium greatly dilutes the secreted EGFP proteins compared to those contained within cells. The levels of fluorescent protein within the medium were thus determined with a fluorescence microtitre plate reader.

3.6 EGFP Concentration Determination

Using a standard curve of the relative fluorescence units (RFU) of known concentrations of recombinant EGFP (rEGFP) protein (Figure 3.9), the amount of EGFP or PTD4-EGFP protein produced by the *Sf*9 cell cultures could be determined. The

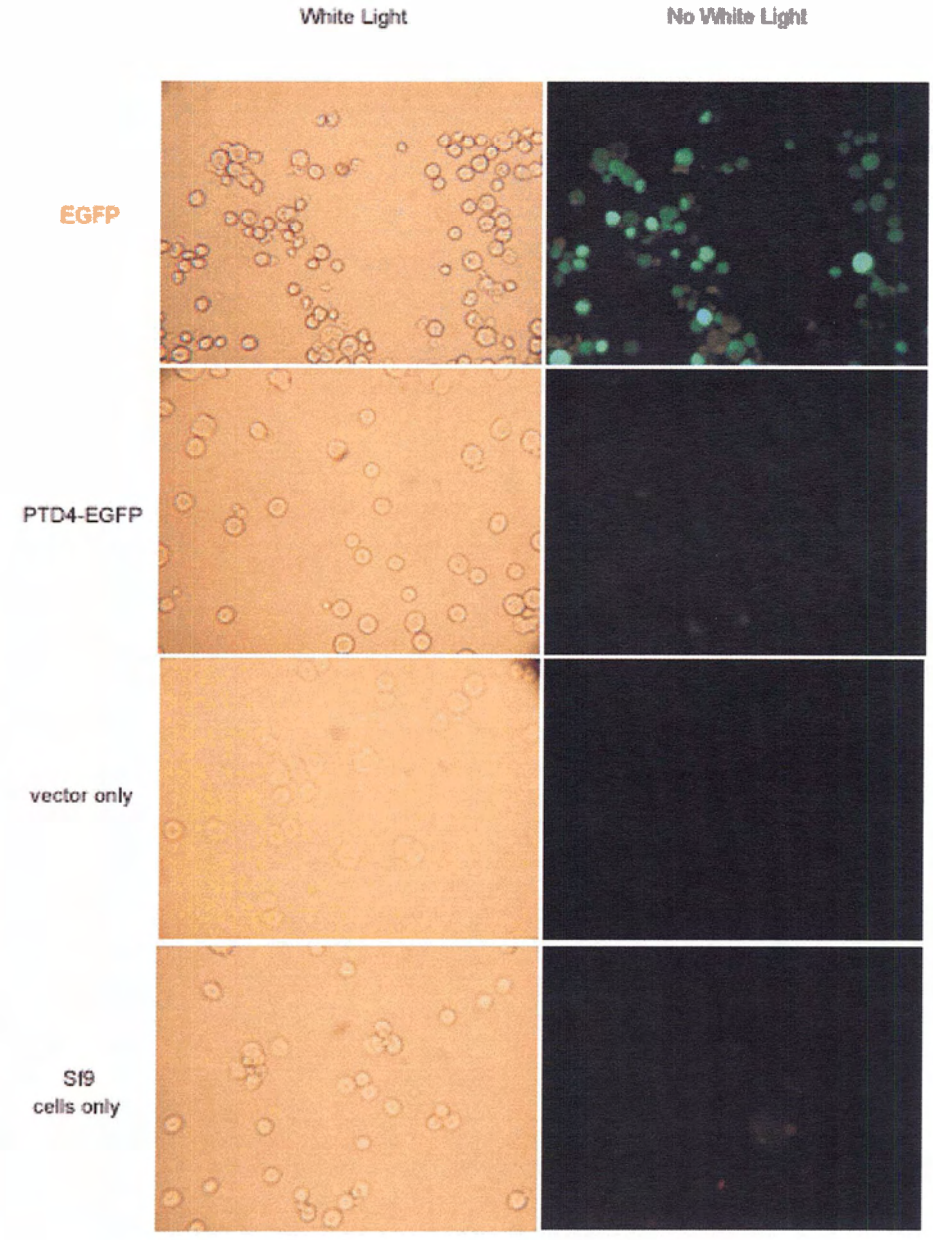

Figure 3.8. Fluorescence micrographs of *Sf*9 cells transfected with p2ZOptcxF-EGFP and p2ZOptcxF-PTD4-EGFP constructs. Visualization was performed using an FITC filter set. Photographs were taken within two minutes of focusing on the field of view to minimize effects of photobleaching. The same field of view was visualized with white light. P2ZOptcxF vector only transfected cells and non-transfected *Sf*9 cells were used as a control.

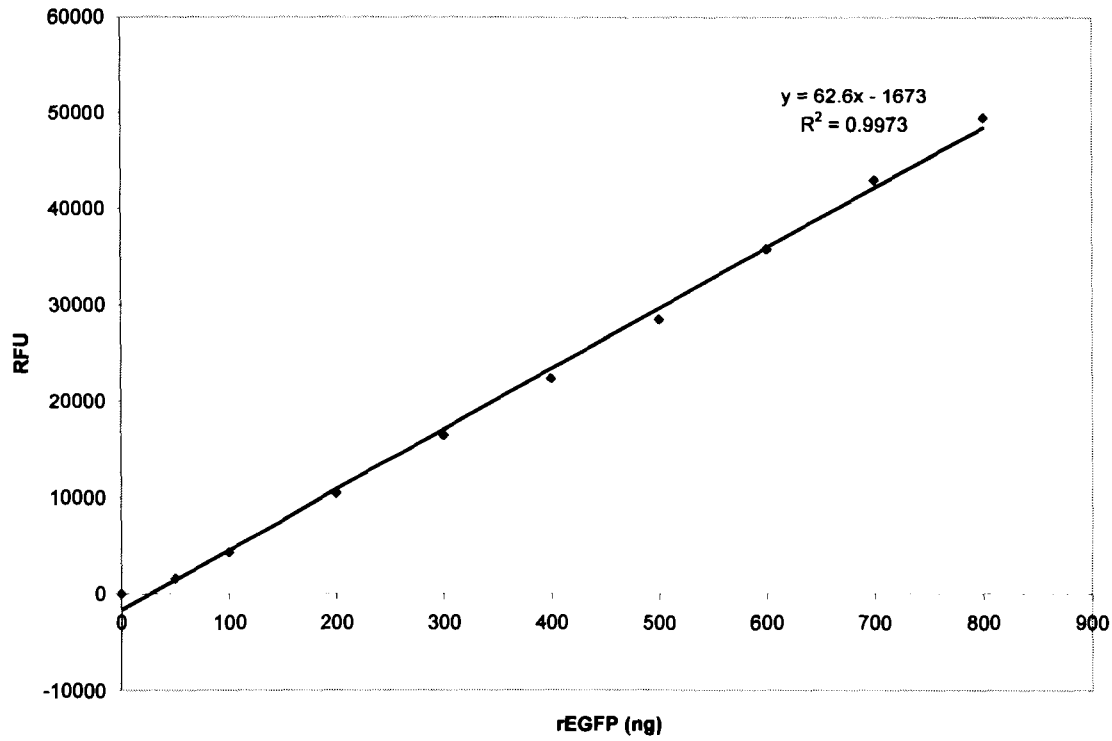

Figure 3.9. Standard curve of recombinant EGFP (rEGFP) protein (Clontech, Palo Alto, CA) quantities (ng) in relation to relative fluorescence units (RFU), to allow determination of EGFP concentration in unknown samples. Fluorescence readings were taken on the Synergy HT-I microtitre plate reader (Biotech, Winooski, VT) with 485/20 excitation and 528/20 emission filter set and a sensitivity setting of 69.

rEGFP standard curve provided an equation of RFU = 62.6(ng of fluorescent protein) - 1673.

For the EGFP cells an average production of 1.2 μg/ml of culture medium was achieved, whereas for the PTD4-EGFP cells an average of 0.9 μg/ml was produced. Keeping in mind that Western blotting (Figure 3.7) revealed the presence of two EGFP cross-reactive species, only a portion of these values was due to the cellulose binding domain tagged proteins. Densitometric analysis of anti-EGFP Western blots was conducted with the Image-Pro Plus analysis software (Media Cybernetics, San Diego, CA). From this analysis it was calculated that approximately 43 % of the anti-EGFP cross-reactive protein secreted into the medium of p2ZOptcxF-EGFP transfected cultures was of the CBD-tagged type. For p2ZOptcxF-PTD4-EGFP transfected cultures, approximately 44 % of the cross-reactive protein was tagged with the CBD (data not shown). Thus the amount of protein of interest produced by the EGFP cells was approximately 0.5 μg/ml and 0.4 μg/ml for the PTD4-EGFP cells.

3.7 GBA Enzyme Activity Assay

To allow determination of the activity of the 4-methyl-umbelliferyl glucopyranoside (4MUGP) artificial substrate assay, the fluorogenic substrate by itself, 4-methyl-umbelliferone (4MU), was used to create a standard curve. Fluorescence at 360 nm excitation and 460 nm emission of 4MU was measured over a linear range (0-20 nmoles) of 4MU quantities (Figure 3.10).

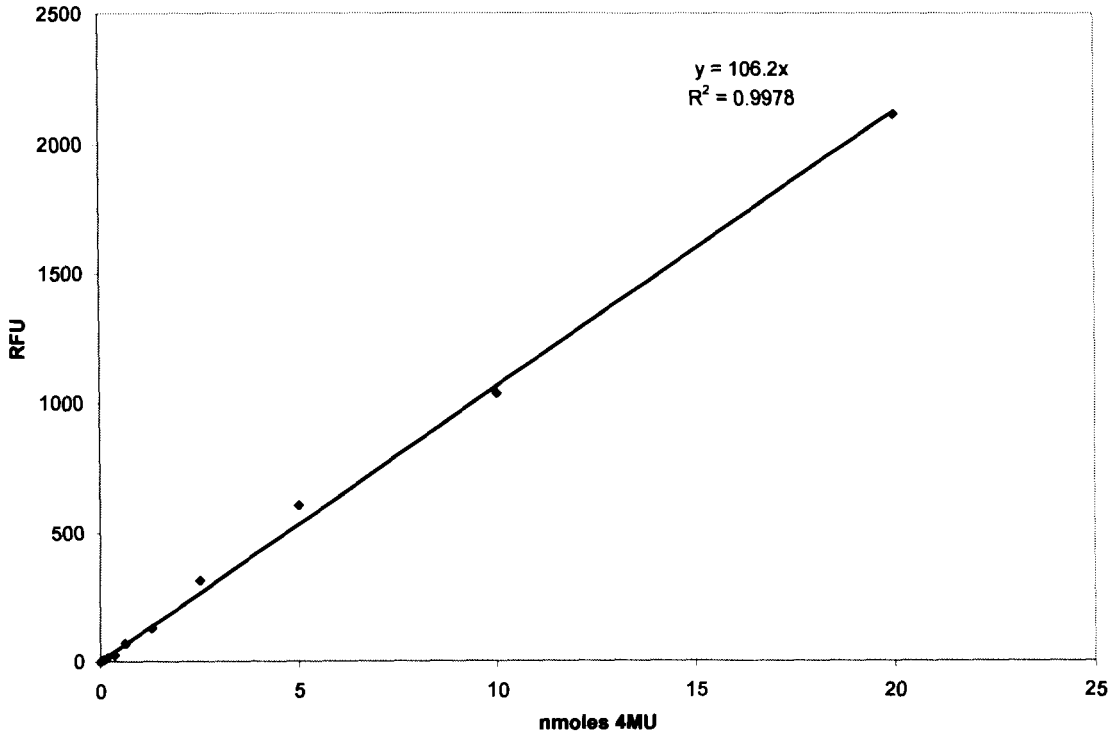

Figure 3.10. Standard curve of relative fluorescence units (RFU) for the fluorogenic substrate 4-methy-umbelliferyl (4MU) in the range of 0-20 nmoles. Fluorescence readings were taken on the Synergy HT-I microtitre plate reader (Biotek, Winooski, VT) with 360/40 excitation and 460/40 emission filter set and a sensitivity setting of 30.

The GBA 4MUGP enzyme activity assay is employed to identify the presence and activity of GBA proteins. Throughout this work, the activity assay resulted in high background levels for the wildtype *Sf*9 control cultures, and low values for p2ZOptcxF-GBA, TAT-GBA and PTD4-GBA transfected cells. Due to the high background levels of 4MUGP cleavage seen for the control cells (Table 3.1), it must be assumed that the TAT-GBA-expressing cells are not producing an active form of the GBA protein, while GBA and PTD4-GBA-expressing cells produce a protein with low levels of activity. Comparison to a known positive control, the 3-1B p2ZOpF-GBA clone, indicates that the expression levels for the p2ZOptcxF-GBA, TAT-GBA and PTD4-GBA transfected cells were very low.

3.8 Concentration of Secreted EGFP and PTD4-EGFP Proteins

Concentration of the secreted proteins of interest with the Amicon stirred cell apparatus resulted in a total 50 fold concentration by volume. In the case of the EGFP-containing proteins the concentration factor could also be monitored by relative fluorescent units. In terms of the fluorescent proteins, the Amicon stirred cell resulted in a concentration factor of 2 fold of fluorescent protein, for every 3.5 fold concentration by volume. The unconcentrated EGFP and PTD4-EGFP initially had fluorescent protein concentrations of 1.2 and 0.9 μg/ml, respectively, and were effectively concentrated to 6.8 μg/ml and 5.3 μg/ml.

Table 3.1. 4-methyl-umbelliferyl glucopyranoside (4MUGP) artificial substrate assay for acid β-glucosidase enzyme produced by stable *Sf*9 transformants. Measurement of cleaved substrate was performed on the Synergy HT-I microtitre plate reader (Biotek, Winooski, VT) with an excitation filter of 360/40 nm, an emission filter of 460/40 nm and a sensitivity setting of 30.

*Sf*9 clone	4MUGP activity[a] (nmol/hr/mg total protein)	Corrected 4MUGP activity[b] (nmol/hr/mg total protein)
Control[c]	1018 +/- 74 (n=21)	–
P2ZOptcxF-GBA	1226 +/- 60 (n=6)	208 +/- 95
P2ZOptcxF-TAT-GBA	1009 +/- 69 (n=6)	-9 +/- 101
P2ZOptcxF-PTD4-GBA	1509 +/- 124 (n=6)	491 +/- 144
3-1B[d] positive control	2360 +/- 78 (n=3)	1342 +/- 108

[a]Activities represent mean values +/- the standard deviation from (n) independent assays.

[b]Specific 4MUGP activity for the untransfected *Sf*9 control cells subtracted from each transfected *Sf*9 clone, to remove the effect of background levels of native *Sf*9 enzyme capable of β-glucosidic linkage cleavage.

[c]Untransfected *Sf*9 cells

[d]p2ZOpF-GBA transfected *Sf*9 clone which is known to express high levels of active GBA, designated as 3-1B (Sinclair 2001)

3.9 Silver Stain and Western Blot Analysis of Cellulose Binding Domain Purified Proteins

Silver stain and Western blot analysis of the proteins that bound to cellulose revealed that the CBD-tagged EGFP-containing fusion proteins were successfully purified to near homogeneity. Silver stain analysis shows proteins of the expected molecular weights for EGFP and PTD4-EGFP prior to and after cleavage of the CBD tag (Figure 3.11A and C). Western blotting shows reactivity with the anti-EGFP antibody for the EGFP-containing proteins (Figure 3.11B and D).

After the medium containing the EGFP and PTD4-EGFP proteins was concentrated, it was adjusted to pH 9.0 and 0.1% TRITON X-100. The addition of 20 mg of Sigmacell™ cellulose resulted in complete binding of the cellulose binding domain (CBD)-tagged proteins during an overnight incubation. All of the CBD-tagged EGFP (Figure 3.11B, Lane 5) and PTD4-EGFP (Figure 3.11D, Lane 6) protein binds to cellulose and none remains in the unbound fraction (Figures 3.11 B and D, Lane 7). Ethylene glycol elution of the bound proteins resulted in approximately 60% recovery of the bound proteins after five washed with ethylene glycol for EGFP (Figure 3.10A, Lane 5). The PTD4-EGFP protein shows better recovery with ethylene glycol elution with approximately 80% removed (Figure 3.11D, Lane 5). The remaining CBD-tagged protein was removed with SDS loading buffer to visualize the amount of protein that remained bound and was not eluted with ethylene glycol (Figure 3.11 A and C, Lane 6).

Factor X_a cleavage of the CBD-tagged EGFP and PTD4-EGFP proteins reveals complete removal of the CBD tag within 24 hours (Figure 3.11A, Lane 8 and C, Lane 9). The Factor X_a Cleavage Capture Kit was 100% effective in removing contaminating

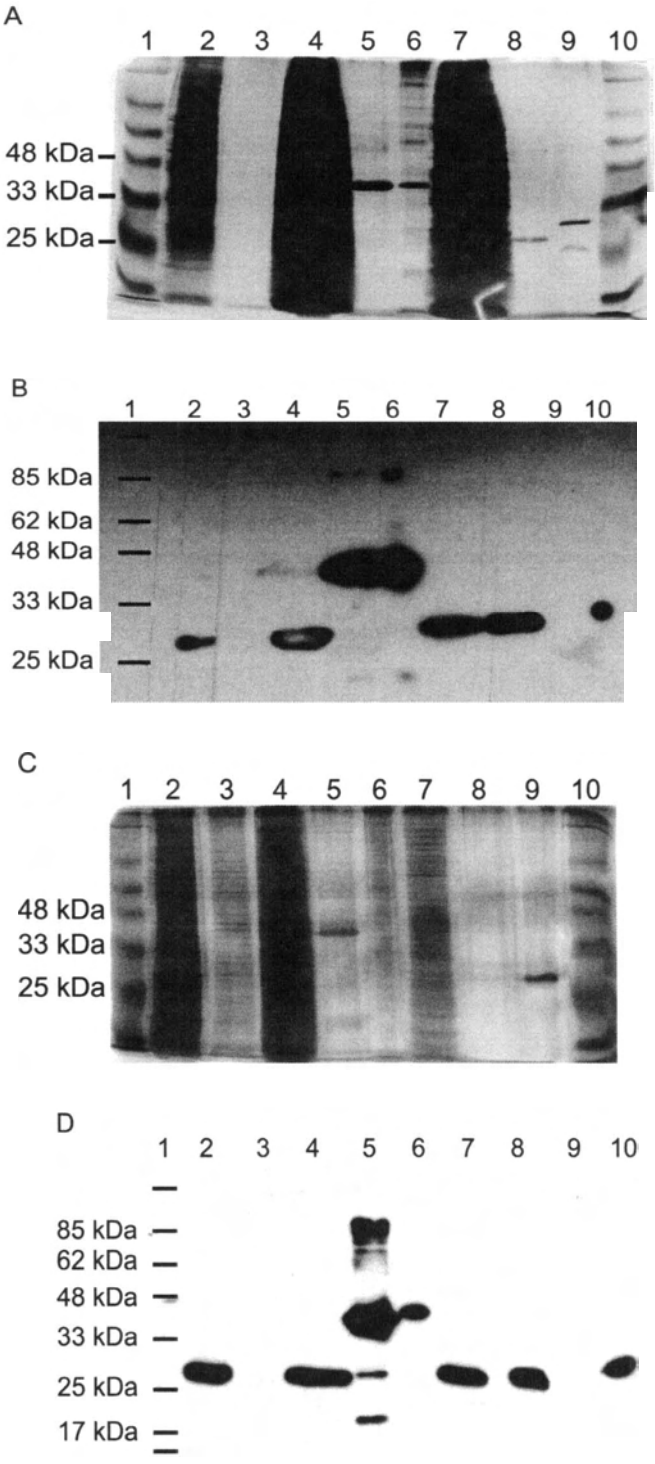

Figure 3.11. Silver stain and Western blot analysis of SDS-PAGE gels of cellulose purified proteins from media of p2ZOPtcxF-EGFP (Panels A and B) and p2ZOPtcxF-PTD4-EGFP (Panels C and D) transfected *Sf*9 cells. In all lanes an equal volume of

sample was loaded to demonstrate the effect of concentration of the crude media. **(A)** Silver stain of proteins secreted to the medium by p2ZOptcxF-EGFP transfected *Sf*9 cells (Lane 2). Crude medium was concentrated with a 10,000 NWML membrane (Millipore, Billerica, MA); the resulting flow through (Lane 3) and concentrated medium (Lane 4) are shown. The concentrated medium was bound to 20 mg of cellulose and bound protein was eluted with 70% ethylene glycol (Lane 5). Any protein remaining bound to cellulose after ethylene glycol elution was removed with SDS-PAGE loading buffer (New England Biolabs, Beverly, MA) (Lane 6) and the unbound proteins are shown in Lane 7. As a control, 0.03 units of Factor X_a were run in Lane 8. Ethylene glycol-eluted EGFP tagged with the cellulose binding domain was cleaved with 0.03 units of Factor X_a overnight, and contaminating Factor X_a was removed with the Novagen Factor X_a Cleavage/Capture kit (EMD Biosciences, San Diego, CA) (Lane 9). Broad Range Protein Standards (New England Biolabs, Beverley, MA) were included as a reference (Lanes 1 and 10). **(B)** Western blot of the above silver stained gel (A) with the same lanes loaded except for Lane 9 which is a blank and Lane 10 which is the recombinant EGFP control protein (Clontech, Palo Alto, CA). **(C)** Silver stain of proteins secreted into the medium by p2ZOptcxF-PTD4-EGFP transfected *Sf*9 cells (Lane 2). Crude medium was concentrated with a 10,000 NWML membrane (Millipore, Billerica, MA); the resulting flow through (Lane 3) and concentrated medium (Lane 4) are shown. The concentrated medium was bound to 20 mg of cellulose and bound protein was eluted with 70% ethylene glycol (Lane 5). Any protein remaining bound to cellulose after ethylene glycol elution was removed with SDS-PAGE loading buffer (New England Biolabs, Beverly, MA) (Lane 6) and the unbound proteins are in Lane 7. Ethylene glycol-eluted PTD4-EGFP tagged with the cellulose binding domain was cleaved with 0.03 units of Factor X_a overnight, and contaminating Factor X_a was removed with the Novagen Factor X_a Cleavage/Capture kit (EMD Biosciences, San Diego, CA) (Lane 8). As a control, 0.03 units of Factor X_a were run in Lane 9. Broad Range Protein Standards (New England Biolabs, Beverley, MA) were included as a reference (Lanes 1 and 10). **(D)** Western blot of the above silver stained gel (C) with the same lanes loaded except for Lane 8 which contains the Factor X_a cleaved PTD4-EGFP protein, Lane 9 which is a blank and Lane 10 which is the recombinant EGFP control protein (Clontech, Palo Alto, CA).

Factor X_a proteins, as demonstrated by the lack of banding at 25 and 30 kDa in Lane 8 of Figures 3.11 A and C, which is present in the Factor X_a control lane (Figure 3.11A, Lane 9).

3.10 Transduction of Sf9 cells with PTD4-EGFP proteins from crude medium

Following the work of Barka *et al.* (2004), wildtype *Sf*9 cells were incubated with PTD4-EGFP proteins present in the crude medium from PTD4-EGFP transfected *Sf*9 cells. As the EGFP proteins have their own inherent fluorescence and do not need to be labeled by fluorescent conjugates, the crude medium without purification of the proteins of interest could be employed. Comparison of control *Sf*9 cells and those incubated with PTD4-EGFP show no appreciable difference in levels of fluorescence at any time point between 10 minutes to 1 hour. It is apparent from trypan blue exclusion that dead *Sf*9 cells exhibit green autofluorescence and cells which present an unhealthy morphology such as bloating or granulation also demonstrated vesicles of green fluorescence (data not shown). Due to these confounding factors, no difference in levels of cellular fluorescence for control *Sf*9 cells, compared to those subjected to EGFP or PTD4-EGFP proteins could be visualized.

4 Discussion

4.1 Plasmid DNA Integration into the Sf9 Insect Genome

Demonstration of the integration of the p2ZOptcxF plasmids containing the fusion genes of interest into the *Sf9* genome, confirmed the success of the transfection procedure. Due to this integration it was assumed that the clones being utilized would be capable of expressing the fusion proteins of interest. *Sf9* cells are capable of accepting multiple insertions into their genomic DNA (Pfeifer, 1998). The number of inserts may be inferred from the intensity of the band produced by the genomic DNA PCR when equal amounts of DNA are used as template for the PCR reaction. In this experiment 150 ng of isolated *Sf9* genomic DNA were used as template for the PCR reaction. The genomic DNA from *Sf9* cells transfected with p2ZOptcxF-EGFP, p2ZOptcxF-PTD4-EGFP and p2ZOptcxF-PTD4-GBA show darker bands than those of p2ZOptcxF-GBA and p2ZOptcxF-TAT-GBA. This may indicate that those cultures selected for use that were transfected with the first three plasmids mentioned, integrated more copies of the plasmid than the latter two. This would indicate that the p2ZOptcxF-EGFP, p2ZOpcxtF-PTD4-EGFP and p2ZOptcxF-PTD4-GBA clones would express the heterologous proteins in greater quantities, which is substantiated by the Western blot analysis of these cultures. An additional method to detect the number of inserts is with Southern blotting which requires the use of radioactively labeled DNA probes complementary to the specific gene insertions of interest. Due to the unavailability of radioactive materials-trained personnel within our laboratory, these tests could not be undertaken at this time. Southern blot analysis would be useful in future study, as it would be beneficial to select

*Sf*9 clones with the greatest number of inserts within their genomic DNA in order to increase the levels of heterologous protein expression.

4.2 Transcription of the Inserted Plasmid DNA

Confirmation of genomic DNA integration of the plasmids, lead to verification of transcription of said insertions. Total RNA extraction, poly-A specific cDNA library construction from reverse transcription of mRNA and gene-specific PCR of the cDNA library were employed. The p2ZOptcxF-GBA, p2ZOptcxF-TAT-GBA and p2ZOptcxF-PTD4-GBA transfected *Sf*9 cultures transcribed mRNAs specific to the GBA gene, while the p2ZOptcxF-EGFP and p2ZOPtcxF-PTD4-EGFP transfected cells had mRNA specific to the EGFP gene. The sense primer bound within the human transferrin secretion signal, while the anti-sense primer bound at the extreme 3' end of the genes of interest. This allowed identification of mRNAs encoding the full-length insert including the secretion signal, cellulose binding domain and genes of interest. As the full length mRNA was present, it was assumed that the protein would be secreted into the medium due to the addition of the human transferrin secretion signal and that the secreted protein could be purified from the culture medium due to the presence of the cellulose binding domain affinity tag.

4.3 Expression of Heterologous Proteins

This study confirms that fact that the *Sf*9 insect system can be used for the expression of heterologous proteins. The EGFP and PTD4-EGFP proteins were produced at levels of 1.2 and 0.9 μg/ml, respectively, which approaches the levels of expression

achieved by Pfeifer *et al.* (1997) and Hegedus *et al.* (1998). This thesis employed an expression vector based on that of the aforementioned investigators, and for a soluble, cytosolic, non-glycosylated protein such as EGFP, acceptable levels of protein could be produced. Complex, highly processed proteins such as Factor X (Pfeifer *et al.*, 2001), melanotransferrin (Hegedus *et al.*, 1999), α3/4 fucosyltransferase III (Morais *et al.*, 2003), and the μ opiod receptor (Kempf *et al.*, 2002) have been expressed in *Sf*9 cells under the *ie*2 promoter which may be a good indication that with proper optimization, this system could be utilized for the expression of more complex proteins such as GBA.

The localization of EGFP and PTD4-EGFP proteins reveals that the human transferrin secretion signal efficiently directs proteins to the culture medium when it remains attached to the heterologous protein. When the EGFP fusion protein undergoes proteolytic cleavage within the cell and the secretion signal is thus removed, the protein is no longer directed to the surrounding medium. Interestingly, when the same proteolysis occurs with the PTD4-EGFP protein, it is still directed to the medium, presumably by the TAT protein transduction domain which has been demonstrated to act as a secretion signal (Xia *et al.*, 2001; Elliger *et al.*, 2002). Secretion of proteins attached to the HIV-I TAT PTD may be affected by the placement of the tag at either the C or N-terminus. Elliger *et al.* (2002) found that C-terminal, but not N-terminal addition of TAT resulted in 10-fold greater secretion of β-glucuronidase, compared to untagged β-glucuronidase. In the case of the p2ZOptcxF-PTD4-EGFP construct, the TAT PTD tag was placed at the N-terminus and thus it appears that placement of the tag and related secretion properties are protein dependent.

Proteolytic cleavage of the CBD tag from the protein of interest has also been experienced in other systems. Ong *et al.* (1991) found that a significant proportion of their β-glucosidase activity did not bind to cellulose as their fusion protein was prone to proteolysis in crude extracts. Upon addition of EDTA, phenylmethylsulfonyl fluoride (PMSF) and pepstatin A, more than 90% of the β-glucosidase activity bound to cellulose. The addition of these or other proteolytic inhibitors to the *Sf*9 culture medium should result in a greater recovery of CBD-tagged EGFP and PTD4-EGFP proteins.

In the case of the GBA-containing proteins it was found that the system produced far less heterologous protein. Protein levels in the low ng/ml range are estimated for the GBA, TAT-GBA and PTD4-GBA proteins. These proteins are large (predicted molecular masses of 79-81 kDa), complex, highly glycosylated, membrane-associated proteins that have been shown to be poorly expressed in other recombinant systems, such as HeLa cells and *Pichia pastoris* (Sinclair, 2001; Campbell, 2003), as well as CHO, human fibroblast and mouse C2C12 cells (Xu *et al.*, 1998).

Due to the apparent small size of the anti-GBA antibody reactive proteins expressed in this work, it is assumed that the GBA proteins produced were not properly glycosylated. The anti-CBD antibody Western blots of the TAT-GBA and PTD4-GBA proteins demonstrated that the small size of these GBA containing proteins is not due to cleavage of the CBD tag at the Factor X_a cleavage site, as these proteins are detectable with the anti-CBD antibody. Despite repeated attempts, the GBA protein could not be detected with the anti-CBD antibody, which may indicate that this protein is produced at levels below the detection limit for the anti-CBD antibody. It may also be the case that this protein has undergone proteolytic cleavage at the Factor X_a cleavage site, resulting in

removal of the CBD tag and thus a lower molecular weight than predicted for the CBD-tagged, glycosylated GBA protein.

In support of the hypothesis that these proteins are unglycosylated or hypoglycosylated, are the low levels of activity detectable by the 4MUGP artificial substrate assay for the GBA enzyme. Glycosylation of GBA at the first of five Asn-X-Ser/Thr positions is required for activity of the enzyme (Grace *et al.*, 1990a; Berg-Fussman *et al.*, 1993). The native human enzyme is glycosylated at four of the five putative glycosylation sites (Berg-Fussman *et al.*, 1993). Expression of a GBA protein in insect cells has demonstrated that the active, glycosylated GBA is 65 kDa (Grabowski *et al.*, 1989; Grace *et al.*, 1990b; Grace *et al.*, 1994; Sinclair, 2001). The addition of the CBD tag should bring the molecular weight of the glycosylated protein to approximately 80 kDa. None of the anti-GBA cross-reactive proteins expressed in this work were detected to be 80 kDa. If sufficient quantities of the GBA-containing fusion proteins could be obtained, deglycosylation of these proteins could be performed with protein N-glycosidase (PNGaseF) following the protocol of Sinclair (2001), to confirm that the GBA, TAT-GBA and PTD4-GBA proteins are hypoglycosylated. At this time, low levels of protein expression prevent this study from being completed.

4.4 Affinity Purification of Heterologous Proteins

The addition of the cellulose binding domain to the proteins of interest was intended to simplify purification of the heterologous proteins away from the other secreted proteins within the *Sf*9 culture medium. For the EGFP-containing proteins the cellulose binding domain could be put to good use and allowed for near homogeneous

purification of the CBD-tagged proteins in one binding and elution step. With the GBA-containing proteins the CBD tag was not effective for purification, as these proteins were expressed at very low levels. Tomme *et al.* (1998) have demonstrated that the kinetics of binding for CBD_{Cex} requires at least a minimum concentration of 1 μM to saturate half of the cellulose binding sites. Even within the more highly expressed EGFP and PTD4-EGFP proteins it was observed that the CBD-tagged EGFP protein which was present at levels of 0.5 μg/ml, was more efficiently and specifically bound, than the CBD-tagged PTD4-EGFP protein, which was present levels of 0.4 μg/ml. For proteins with expression levels in the low ng/ml range, like GBA, TAT-GBA and PTD4-GBA, unfavorable kinetics do not allow efficient purification and lead to high levels of non-specific binding of other *Sf*9 native proteins (data not shown). This indicates that competitive binding occurs with the CBD-tagged proteins and that with higher levels of CBD-tagged proteins, there are fewer chances for non-specific binding of other untagged proteins.

Comparison to the work of Sinclair (2001), which employed the p2ZOpF insect expression vector, on which the p2ZOptcxF vector for expression of GBA is based, shows that the *Sf*9 insect system is capable of expressing GBA in μg/ml quantities. Due to the marked decrease in expression levels for the CBD-tagged GBA control protein expressed in this work, it appears that the addition of the 14 kDa CBD affinity purification tag imparts a translational difficulty to the *Sf*9 expression system. The addition of this large tag at the N-terminus of the GBA protein may not only inhibit protein translation but also proper glycosylation of the GBA enzyme, resulting in the production on an enzymatically inactive protein. With this in mind, it may be beneficial to redesign the p2ZOptcxF vector to remove the N-terminal CBD region and add an N- or

C-terminal affinity purification tag of a smaller size. Work by Wei in our laboratory (unpublished data) has shown that the addition of a poly-histidine tag to the C-terminus of the GBA protein results in production of an inactive enzyme. The intervening sequence of the TAT transduction domain may allow production of an active GBA enzyme with an N-terminal poly-histidine tag and could be engineered with a proteolytic cleavage site to allow its removal after purification. Alternatively, use of another small affinity tag such as Strep- or FLAG- tags could be attempted as they allow purification of active fusion proteins under non-denaturing conditions (Terpe, 2003).

4.5 Transduction of HIV-1 TAT Tagged Proteins

The EGFP and PTD4-EGFP proteins produced by the insect cell expression system have their own inherent fluorescence label and thus need not be labelled with FITC or other markers to allow for their visualization by epi-fluorescence microscopy. Barka *et al.* demonstrated that Chinese hamster ovary (CHO)-secreted green fluorescent protein fused to TAT could be used directly for transduction into control CHO cells. This method was attempted with the medium from PTD4-EGFP expressing *Sf*9 cultures on wildtype *Sf*9 cells but no transduction could be visualized. A number of theories as to why transduction was unsuccessful can be envisioned.

It is possible that the N-terminal CBD tag on the PTD4-EGFP fusion protein may effectively block the transduction abilities of the PTD4 domain. As the CBD tag is intended to be removed from the fusion protein prior to transduction, the method of Barka *et al.* may not be appropriate in this system. Schwarze *et al.* (2000a) predict that as long as the TAT PTD is not buried internally, efficient transduction will occur. Of note is

the position of the PTD at amino acid residues 47-57 within the native HIV-I TAT protein (Vives *et al.*, 1997a). This may indicate that the TAT PTD is capable of transducing proteins when it is embedded within the protein backbone. No studies to date have attempt the placement of the TAT PTD within a protein or between two protein domains, so the effect of placing the TAT PTD between the CBD and EGFP domains is not easily predicted. Future work will be directed at purifying sufficient amounts of the PTD4-EGFP protein which has the CBD tag removed to allow transduction studies.

If the TAT protein does indeed require heparan sulfate surface molecules for internalization as postulated by Tyagi *et al.* (2001), it may be possible that *Sf*9 cells do not express heparan sulfate and thus cannot take up protein transduction domain-tagged fusion proteins. A lack of heparin sulfate proteoglycans on the surface of *Sf*9 cells does not seem likely though, as many studies in *Drosophila melanogaster*, a dipteran insect, have shown their presence on most cells (Seppo *et al.*, 2000; Princivalle *et al.*, 2002).

In the likely event that *Sf*9 cells express heparan sulfate surface molecules, one confounding factor in these experiments may include the fact that certain cell types do not allow protein transduction. To date, Madin-Darby canine kidney (MDCK) renal epithelial (Violini *et al.*, 2002; Kramer *et al.*, 2003) and CaCo-2 colonic carcinoma cells (Violini *et al.*, 2002), despite the expression of heparan sulfate proteoglycans, show no transduction. In addition, the degree of internalization of PTD-tagged proteins is cell-type dependent and different variations on the amino acid sequence of the PTD effect uptake in various cell-types (Mai *et al.*, 2002).

Interestingly, transduction of a correctly folded TAT-GFP fusion protein into cells results in a high intracellular level of TAT-GFP but with a significant loss of GFP

emission (A. Vocero-Akbani, A. Ho and S.F. Dowdy, unpublished, in Schwarze *et al.*, 2000b). These observations suggest that transduction across the cellular membrane requires partial or complete unfolding of the protein which then needs to be refolded *in vivo*. Park *et al.*(2000) have also demonstrated that a denatured TAT-GFP protein is transduced more efficiently than the native form. The same phenomenon may be occurring in insect cells, though the level of transduced but inactive EGFP was not determined in this study.

This work employed the use of living, non-fixed cells for fluorescence microscopy analysis, as the use of fixation has been implicated in artifactual redistribution of PTD-containing proteins. Leifert *et al.* (2002; 2003), Lundberg *et al.* (2002) and Richards *et al.* (2003) have demonstrated that the use of methanol, in particular and also milder fixatives such as paraformaldehyde and acetone cause cellular membrane disruption, allowing surface-bound PTD proteins to be localized to the nucleus and cytoplasm. If the same experiments are performed on living cells, the level of transduction is greatly diminished and appears to be localized to endosomes, supporting an endocytotic mode of transduction.

Several studies have also started to employ stains that recognize living from dead cells to ensure that transduction not only occurs by the passage of PTD proteins into dead, permeabilized cells (Mai *et al.*, 2002; Kramer *et al.*, 2003; Richard *et al.*, 2003). In this work, trypan blue exclusion was used to identify dead from living cells. In the case of *Sf*9 cells it was observed that cells that stain with trypan blue do exhibit green autofluorescence. This autofluorescence is present in cultures incubated with PTD4-EGFP as well as those incubated with EGFP or with regular medium. In addition, cells

with an unhealthy morphology (bloating, granulation) also exhibit green fluorescence in small vesicles, regardless of whether or not they were incubated with the PTD4-EGFP protein, which highlights further artifactual data that could be confused as transduction of PTD4-EGFP proteins via an endocytotic pathway. From this microscopic analysis it is clear that careful preparation and examination of cells for transduction studies is required to ensure that no artifactual data are misconstrued as transduction of PTD-containing proteins.

5 Conclusions and Future Directions

This thesis has addressed the issue of TAT fusion protein expression in the *Sf*9 insect cell expression system. Expression of soluble, non-glycosylated, cellulose binding domain-tagged proteins such as enhanced green fluorescent protein can be achieved. At this time, the *Sf*9 expression system did not to allow for sufficient levels of expression of the complex, highly glycosylated, CBD-tagged acid β-glucosidase proteins. It appears that the addition of the CBD tag may allow simplified purification if high levels of protein are expressed, but its addition also lowers the levels of protein expression overall. In this regard a smaller, more easily translated affinity purification tag such as poly-histidine may be indicated.

This work employed polyclonal, transfected *Sf*9 cultures as selection of clonal lines was thought to be difficult in *Sf*9 cells, due to their dependence on cell-cell interaction for growth. Invitrogen (Burlington, ON) now publishes a clonal selection guide for *Sf*9 cells, which could allow the selection of more consistent, highly expressing clones. Screening of a number of clones for those with the best expression levels may allow selection of clones with the desired 1-9 μg/ml heterologous protein expression levels published by Pfeifer *et al.* (2001) and Hegedus *et al.* (1999)

Finally, further scale-up of expression cultures may be required to obtain sufficient levels of TAT-fusion proteins to allow fluorescent labeling of the proteins and subsequent transduction studies. Sinclair (2001) acknowledges the assistance of Dr. T. Pfeifer (University of British Columbia, Vancouver, BC) for expression of high levels of acid β-glucosidase expression in *Sf*9 insect cells. These expression methods (unpublished) could be applied to CBD-tagged TAT fusion proteins to increase

production levels, and allow purification of μg/ml quantities of heterologous protein. For expression of Factor X proteins, Pfiefer *et al.* (2001) scaled their shake flask cultures to 2 litre fermentation cultures, which resulted in a doubling of the heterologous protein output (18 μg/ml) as compared to 20 ml shake flask culture (9 μg/ml).

A variety of steps aimed at increasing the level of protein expression of the GBA-containing proteins will be required to test the transduction abilities of a TAT-GBA fusion protein. Once sufficient levels of protein are expressed and purified, it will be important to study transduction on living, non-fixed cells in order to prevent the introduction of artifacts due to permeablization of the cell membrane. The use of sodium azide or 4°C incubation to inhibit energy-dependent endocytosis, and heparan sulfate deficient cells would be of interest to further elucidate the mode of transport of TAT-PTD fusion proteins, and in particular a TAT-GBA fusion.

Potential use of purified, TAT and PTD4-tagged GBA proteins for enzyme replacement therapy of Gaucher disease could be tested by transducing both normal and Gaucher cell lines. The ability of these tagged proteins to cross the blood brain barrier could also be studied in a mouse model of Gaucher disease, which is currently being created by Dr. Graham Sinclair (UBC, Vancouver, BC). If transduction of the TAT-GBA fusion proteins is successful, patients with Gaucher disease could benefit from an enzyme replacement therapy that is more readily taken up by all cells of the body and particularly those of the brain and central nervous system.

6 References

Aerts, J. M., W. E. Donker-Koopman, C. van Laar, S. Brul, G. J. Murray, D. A. Wenger, J. A. Barranger, J. M. Tager and A. W. Schram (1987). Relationship between the two immunologically distinguishable forms of glucocerebrosidase in tissue extracts. *Eur J Biochem* 163(3): 583-589.

Albini, A., R. Benelli, M. Presta, M. Rusnati, M. Ziche, A. Rubartelli, G. Paglialunga, F. Bussolino and D. Noonan (1996a). HIV-tat protein is a heparin-binding angiogenic growth factor. *Oncogene* 12(2): 289-297.

Albini, A., R. Soldi, D. Giunciuglio, E. Giraudo, R. Benelli, L. Primo, D. Noonan, M. Salio, G. Camussi, W. Rockl and F. Bussolino (1996b). The angiogenesis induced by HIV-1 tat protein is mediated by the Flk-1/KDR receptor on vascular endothelial cells. *Nature Medicine* 2(12): 1371-1375.

Ali, S. A., H. C. Joao, R. Csonga, F. Hammerschmid and A. Steinkasserer (1996). High-yield production of functionally active human serum transferrin using a baculovirus expression system, and its structural characterization. *Biochemistry Journal* 319 (Pt 1): 191-195.

Altmann, F., E. Staudacher, I. B. Wilson and L. Marz (1999). Insect cells as hosts for the expression of recombinant glycoproteins. *Glycoconjugate Journal* 16(2): 109-123.

Arya, S. K., C. Guo, S. F. Josephs and F. Wong-Staal (1985). Trans-activator gene of human T-lymphotropic virus type III (HTLV-III). *Science* 229(4708): 69-73.

Assouline, Z., R. Graham, R. C. Miller, Jr., A. J. Warren and D. G. Kilburn (1995). Processing of fusion proteins with immobilized factor Xa. *Biotechnology Progress* 11(1): 45-49.

Assouline, Z., H. Shen, D. Kilburn and R. A. J. Warren (1993). Production and properties of a factor X-cellulose-binding domain fusion protein. *Protein Engineering* 6(7): 787-792.

Barka, T., E. S. Gresik and S. C. Henderson (2004). Production of cell lines secreting TAT fusion proteins. *J Histochem Cytochem* 52(4): 469-477.

Barranger, J. A., J. Tomich, S. Weiler, S. Sakallah, C. Sansieri, T. Mifflin, A. Bahnson, F. S. Wei, J. F. Wei and M. Vallor (1995). Molecular biology of glucocerebrosidase and the treatment of Gaucher disease. *Cytokines and Molecular Therapies* 1: 149-163.

Bayer, P., M. Kraft, A. Ejchart, M. Westendorp, R. Frank and P. Rosch (1995). Structural studies of HIV-1 Tat protein. *Journal of Molecular Biology* 247(4): 529-535.

Becker-Hapak, M., S. S. McAllister and S. F. Dowdy (2001). TAT-mediated protein transduction into mammalian cells. *Methods* 24: 247-256.

Bennett, R. P., B. Dalby and P. M. Guy (2002). Protein delivery using VP22. *Nature Biotechnology* 20(1): 20.

Berg-Fussman, A., M. E. Grace, Y. Ioannou and G. A. Grabowski (1993). Human Acid beta-Glucoisdase. N-glycosylation site occupancy and the effect of glycosylation on enzymatic activity. *The Journal of Biological Chemistry* 268(20): 14861-14866.

Beutler, E. (1997). Enzyme replacement therapy for Gaucher's disease. *Baillieres Clin Haematol* 10(4): 751-763.

Beutler, E. and T. Gelbart (1998). Hematologically important mutations: Gaucher Disease. *Blood Cells Molecules and Diseases* 24: 2-8.

Beutler, E. and G. A. Grabowski (2001). Gaucher Disease. *The Metabolic and Molecular Bases of Inherited Disease.* D. Valle. New York, McGraw Hill. 3: 3635-3668.

Beutler, E., N. Nguyen, M. Henneberger, J. Smolec, R. McPherson, C. West and T. Gelbart (1993). Gaucher disease: gene frequencies in the Askenazi Jewish population. *American Journal of Human Genetics* 52: 85-88.

Bonifaci, N., R. Sitia and A. Rubartelli (1995). Nuclear translocation of an exogenous fusion protein containing HIV Tat requires unfolding. *AIDS* 9: 995-1000.

Bradford, M. M. (1976). A rapid and sensitive method for the quantitation of microgram quantities of protein utilizing the principle of protein-dye binding. *Analytical Biochemistry* 72: 248-254.

Brady, R., G. Murray and N. Barton (1997). Glucosylceramide lipidosis: Gaucher disease. *The Molecular and Genetic Basis of Neurological Disease.* R. Barchi. Boston, Butterworth Heinemann: 405-420.

Brady, R. O., J. Kanfer and D. Shapiro (1965a). The Metabolism of Glucocerebrosides. I. Purification and Properties of a Glucocerebroside-Cleaving Enzyme from Spleen Tissue. *Journal of Biological Chemistry* 240: 39-43.

Brady, R. O., J. N. Kanfer and D. Shapiro (1965b). Metabolism of Glucocerebrosides. Ii. Evidence of an Enzymatic Deficiency in Gaucher's Disease. *Biochemical and Biophysical Research Communications* 18: 221-225.

Burns, G., R. Cawley, R. Flemans, K. Higgy and C. Worman (1977). Surface marker and other characteristics of Gaucher's cell. *Journal of Clinical Pathology* 30: 981.

Calmels, T., M. Parriche, H. Durand and G. Tiraby (1991). High Efficiency Transformation of Tolypocladium geodes Conidiospores to Phleomycin Resistance. *Current Genetics* 20: 309-314.

Campbell, T. N. (2003). Glucocerebrosidase Expression and Analysis. *Department of Biology*. Victoria, BC, University of Victoria: 115.

Cao, G., W. Pei, H. Ge, Q. Liang, Y. Luo, F. R. Sharp, A. Lu, R. Ran, S. H. Graham and J. Chen (2002). In Vivo Delivery of a Bcl-xL Fusion Protein Containing the TAT Protein Transduction Domain Protects against Ischemic Brain Injury and Neuronal Apoptosis. *Journal of Neuroscience* 22(13): 5423-5431.

Chazenbalk, G. and B. Rapaport (1995). Expression of the extracellular domain of the thyrotropin receptor in the baculovirus system using a promoter active earlier than the polyhedrin promoter. *Jounal of Biologial Chemistry* 270: 1543-1549.

Choy, F. Y. (1984). Gaucher disease: the effects of phosphatidylserine on glucocerebrosidase from normal and Gaucher fibroblasts. *Hum Genet* 67(4): 432-436.

Churcher, M. J., C. Lamont, F. Hamy, C. Dingwall, S. M. Green, A. D. Lowe, J. G. Butler, M. J. Gait and J. Karn (1993). High affinity binding of TAR RNA by the human immunodeficiency virus type-1 tat protein requires base-pairs in the RNA stem and amino acid residues flanking the basic region. *Journal of Molecular Biology* 230(1): 90-110.

Cody, C. W., D. C. Prasher, W. M. Westler, F. G. Prendergast and W. W. Ward (1993). Chemical-Structure of the Hexapeptide Chromophore of the Aequorea Green-Fluorescent Protein. *Biochemistry* 32(5): 1212-1218.

Cormack, B. P., R. H. Valdivia and S. Falkow (1996). FACS-optimized mutants of the green fluorescent protein (GFP). *Gene* 173(1 Spec No): 33-38.

Creagh, A. L., E. Ong, E. Jervis, D. G. Kilburn and C. A. Haynes (1996). Binding of the cellulose-binding domain of exoglucanase Cex from Cellulomonas fimi to insoluble microcrystalline cellulose is entropically driven. *Proceedings of the National Academy of Science U S A* 93: 12229-12234.

Derossi, D., S. Calvet, A. Trembleau, A. Brunissen, G. Chassaings and A. Prochiantz (1996). Cell internalization of the third helix of Antennapedia homeodomain is receptor-independent. *Journal of Biological Chemistry* 271(30): 18188-18193.

Derossi, D., A. H. Joliot, G. Chassaings and A. Prochiantz (1994). The third helix of the Antennapedia homeodomain translocates through biological membranes. *Journal of Biological Chemistry* 269(14): 10444-10450.

Dietz, G. P., E. Kilic and M. Bahr (2002). Inhibition of neuronal apoptosis in vitro and in vivo using TAT-mediated protein transduction. *Molecular and Cellular Neuroscience* 21(1): 29-37.

Dowdy, S. F. (2000). Protein transduction: delivery of TAT-fusion proteins into mammalian cells. St. Louis, Howard Hughes Medical Institute Departments of Pathology and Medicine: 1-10.

Egleton, R. D. and T. P. Davis (1997). Bioavailability and transport of peptides and peptide drugs into the brain. *Peptides* 18(9): 1431-1439.

Elliger, S. S., C. A. Elliger, C. Lang and G. L. Watson (2002). Enhanced secretion and uptake of beta-glucuronidase improves adeno-associated viral-mediated gene therapy of mucopolysaccharidosis type VII mice. *Molecular Therapy* 5(5 Pt 1): 617-626.

Embury, J., D. Klein, A. Pileggi, M. Ribeiro, S. Jayaraman, R. D. Molano, C. Fraker, N. Kenyon, C. Ricordi, L. Inverardi and R. L. Pastori (2001). Proteins linked to a protein transduction domain efficiently transduce pancreatic islets. *Diabetes* 50: 1706-1713.

Ensoli, B., L. Buonaguro, G. Barillari, V. Fiorelli, R. Gendelamn, R. A. Morgan, P. Wingfield and R. C. Gallo (1993). Release, uptake and effects of extracellular human immunodeficiency virus type 1 tat protein on cell growth and viral transactivation. *Jounral of Virology* 67(1): 277-287.

Ezhevsky, S. A., H. Nagahara, A. M. Vocero-Akbani, D. R. Gius, M. C. Wei and S. F. Dowdy (1997). Hypo-phosphorylation of the retinoblastoma protein (pRb) by cyclin D:Cdk4/6 complexes results in active pRb. *Proceedings of the National Academy of Science U S A* 94(20): 10699-10704.

Fabrega, S., P. Durand, P. Codogno, C. Bauvy, C. Delomenie, B. Henrissat, B. M. Martin, C. McKinney, E. I. Ginns, J. P. Mornon and P. Lehn (2000). Human glucocerebrosidase: heterologous expression of active site mutants in murine null cells. *Glycobiology* 10(11): 1217-1224.

Fawell, S., J. Seery, Y. Daikh, C. Moore, L. L. Chen, B. Pepinsky and J. Barsoum (1994). Tat-mediated delivery of heterologous proteins into cells. *Proceedings of the National Academy of Science USA* 91: 664-668.

Ferrari, A., V. Pellegrini, C. Arcangeli, A. Fittipaldi, M. Giacca and F. Beltram (2003). Caveolae-mediated internalization of extracellular HIV-1 tat fusion proteins visualized in real time. *Molecular Therapy* 8(2): 284-294.

Fittipaldi, A., A. Ferrari, M. Zoppe, C. Arcangeli, V. Pellegrini, F. Beltram and M. Giacca (2003). Cell membrane lipid rafts mediate caveolar endocytosis of HIV-1 Tat fusion proteins. *Journal of Biological Chemistry* 278(36): 34141-34149.

Frankel, A. D., S. Biancalana and D. Hudson (1989). Activity of synthetic peptides from the Tat protein of human immunodeficiency virus type 1. *Proceedings of the National Academy of Science U S A* 86(19): 7397-7401.

Frankel, A. D. and C. O. Pabo (1988). Cellular uptake of the Tat protein from Human Immunodeficiency Virus. *Cell* 55: 1189-1193.

Frankel, A. D. and J. A. Young (1998). HIV-1: fifteen proteins and an RNA. *Annual Review of Biochemistry* 67: 1-25.

Friedman, B., K. Vaddi, C. Preston, E. Mahon, J. R. Cataldo and J. M. McPherson (1999). A comparison of the pharmacological properties of carbohydrate remodeled recombinant and placental-derived beta-glucocerebrosidase: implications for clinical efficacy in treatment of Gaucher disease. *Blood* 93(9): 2807-2816.

Fujiwara, T., T. Yamamori and K. Akagawa (2001). Suppresion of transmitter release by Tat HPC-1/syntaxin iA fusion protein. *Biochimica et Biophysica Acta* 1539: 225-232.

Furbish, F. S., C. J. Steer, N. L. Krett and J. A. Barranger (1981). Uptake and distribution of placental glucocerebrosidase in rat hepatic cells and effects of sequential deglycosylation. *Biochimica et Biophysica Acta* 673(4): 425-434.

Futaki, S., T. Suzuki, W. Ohashi, T. Yagami, S. Tanaka, K. Ueda and Y. Sugiura (2001). Arginine-rich peptides. An abundant source of membrane-permeable peptides having potential as carriers for intracellular protein delivery. *Journal of Biological Chemistry* 276: 5836-5840.

Gilkes, N., B. Henrissat, D. Kilburn, D. Miller, R. J. Miller and R. Warren (1991). Domains in Microbial beta-1,4-Glycanases: Sequence Conservation, Function, and Enzyme Families. *Microbiological Reviews* 55(2): 303-315.

Ginns, E. I., R. O. Brady, S. Pirruccello, C. Moore, S. Sorrell, F. S. Furbish, G. J. Murray, J. Tager and J. A. Barranger (1982). Mutations of glucocerebrosidase: discrimination of neurologic and non-neurologic phenotypes of Gaucher disease. *Proc Natl Acad Sci U S A* 79(18): 5607-5610.

Grabowski, G. A., W. R. White and M. E. Grace (1989). Expression of functional human acid beta-glucosidase in COS-1 and Spodoptera frugiperda cells. *Enzyme* 41(3): 131-142.

Grace, M. E. and G. A. Grabowski (1990a). Human acid beta-glucosidase: glycosylation is required for catalytic activity. *Biochemical and Biophysical Research Communications* 168(2): 771-777.

Grace, M. E., P. N. Graves, F. I. Smith and G. A. Grabowski (1990b). Analyses of catalytic activity and inhibitor binding of human acid beta-glucosidase by site-directed mutagenesis. Identification of residues critical to catalysis and evidence for causality of

two Ashkenazi Jewish Gaucher disease type 1 mutations. *J Biol Chem* 265(12): 6827-6835.

Grace, M. E., K. M. Newman, V. Scheinker, A. Berg-Fussman and G. A. Grabowski (1994). Analysis of human acid beta-glucosidase by site-directed mutagenesis and heterologous expression. *J Biol Chem* 269(3): 2283-2291.

Green, M. and P. M. Loewenstein (1988). Autonomous functional domains of chemically synthesized Human Immunodeficiency Virus Tat trans-activator protein. *Cell* 55: 1179-1188.

Greenwood, J., N. R. Gilkes, D. Kilburn, R. J. Miller and R. A. J. Warren (1989). Fusion to an endoglucanase allows alkaline phosphatase to bind to cellulose. *FEBS Letters* 244(1): 127-131.

Guarna, M. M., H. C. Cote, E. M. Kwan, G. L. Rintoul, B. Meyhack, J. Heim, R. T. MacGillivray, R. A. Warren and D. G. Kilburn (2000). Factor X fusion proteins: improved production and use in the release in vitro of biologically active hirudin from an inactive alpha-factor-hirudin fusion protein. *Protein Expr Purif* 20(2): 133-141.

Hallbrink, M., A. Floren, A. Elmquist, M. Pooga, T. Bartfai and U. Langel (2001). Cargo delivery kinetics of cell-penetrating peptides. *Biochimica et Biophysica Acta* 1515(2): 101-109.

Hegedus, D. D., T. A. Pfeifer, J. Hendry, D. A. Theilmann and T. A. Grigliatti (1998). A series of broad host range shuttle vectors for constitutive and inducible expression of heterologous proteins in insect cell lines. *Gene* 207: 241-249.

Hegedus, D. D., T. A. Pfeifer, D. A. Theilmann, M. L. Kennard, R. Gabathuler, W. A. Jefferies and T. A. Grigliatti (1999). Differences in the expression and localization of human melanotransferrin in lepidopteran and dipteran insect cell lines. *Protein Expr Purif* 15(3): 296-307.

Ho, A., S. R. Schwarze, S. J. Mermelstein, G. Waksman and S. F. Dowdy (2001). Synthetic protein transduction domains: enhanced transduction potential *in vitro* and *in vivo*. *Cancer Research* 61: 474-477.

Hollister, J., E. Grabenhorst, M. Nimtz, H. Conradt and D. L. Jarvis (2002). Engineering the Protein N-glycosylation Pathway in Insect Cells for Production of Biantennary, Complex N-glycans. *Biochemistry* 41: 15093-15104.

Horowitz, M., S. Wilder, J. Keesey, M. Leous, R. von Miltenburg and C. Schroeder (1989). The human glucocerebrosidase gene and pseudogene: structure and evolution. *Genomics* 4: 87-96.

Horowitz, M. and A. Zimran (1994). Mutations causing Gaucher disease. *Human Mutation* 3(1): 1-11.

Hubbard, A. L. and H. Stukenbrok (1979a). An electron microscope autoradiographic study of the carbohydrate recognition systems in rat liver. II. Intracellular fates of the 125I-ligands. *Journal of Cell Biology* 83(1): 65-81.

Hubbard, A. L., G. Wilson, G. Ashwell and H. Stukenbrok (1979b). An electron microscope autoradiographic study of the carbohydrate recognition systems in rat liver. I. Distribution of 125I-ligands among the liver cell types. *Journal of Cell Biology* 83(1): 47-64.

Jarvis, D. L. (1993). Foreign gene expression in insect cells. *Insect Cell Culture Engineering.* P. Faulkner. New York, NY, Marcel Dekker: 195-219.

Jarvis, D. L., C. Weinkauf and L. A. Guarino (1996). Immediate-early baculovirus vectors for foreign gene expression in transformed or infected insect cells. *Protein Expression and Purification* 8(2): 191-203.

Kempf, J., L. A. Snook, J. L. Vonesch, T. E. Dahms, F. Pattus and D. Massotte (2002). Expression of the human mu opioid receptor in a stable Sf9 cell line. *Journal of Biotechnology* 95(2): 181-187.

Kilic, E., G. P. Dietz, D. M. Hermann and M. Bahr (2002). Intravenous TAT-Bcl-Xl is protective after middle cerebral artery occlusion in mice. *Annals of Neurology* 52(5): 617-622.

Kilic, U., E. Kilic, G. P. Dietz and M. Bahr (2003). Intravenous TAT-GDNF is protective after focal cerebral ischemia in mice. *Stroke* 34(5): 1304-1310.

Kramer, S. D. and H. Wunderli-Allenspach (2003). No entry for TAT(44-57) into liposomes and intact MDCK cells: novel approach to study membrane permeation of cell-penetrating peptides. *Biochim Biophys Acta* 1609(2): 161-169.

Leifert, J. A., S. Harkins and J. L. Whitton (2002). Full-length proteins attached to the HIV tat protein transduction domain are neither transduced between cells, nor exhibit enhanced immunogenicity. *Gene Ther* 9(21): 1422-1428.

Leifert, J. A. and J. L. Whitton (2003). "Translocatory proteins" and "protein transduction domains": a critical analysis of their biological effects and the underlying mechanisms. *Mol Ther* 8(1): 13-20.

Li, E., S. L. Brown, C. S. Dolman, G. B. Brown and G. R. Nemerow (2001). Production of functional antibodies generated in a nonlytic insect cell expression system. *Protein Expression and Purification* 21(1): 121-128.

Liu, Y., M. Jones, C. M. Hingtgen, G. Bu, N. Laribee, R. E. Tanzi, R. D. Moir, A. Nath and J. J. He (2000). Uptake of HIV-1 tat protein mediated by low-density lipoprotein receptor-related protein disrupts the neuronal metabolic balance of the receptor ligands. *Nature Medicine* 6(12): 1380-1387.

Luckow, V. A. and M. D. Summers (1989). High level expression of nonfused foreign genes with Autographa californica nuclear polyhedrosis virus expression vectors. *Virology* 170(1): 31-39.

Lundberg, M. and M. Johansson (2002). Positively charged DNA-binding proteins cause apparent cell membrane translocation. *Biochem Biophys Res Commun* 291(2): 367-371.

Maeda, S. (1989). Expression of foreign genes in insects using baculovirus vectors. *Annual Review of Entomology* 34: 351-372.

Mai, J. C., H. Shen, S. C. Watkins, T. Cheng and P. D. Robbins (2002). Efficiency of protein transduction is cell type-dependent and is enhanced by dextran sulfate. *J Biol Chem* 277(33): 30208-30218.

Mann, D. A. and A. D. Frankel (1991). Endocytosis and targeting of exogenous HIV-1 Tat protein. *European Molecular Biology Organization (EMBO) Journal* 10(7): 1733-1739.

Miao, S., J. D. McCarter, M. E. Grace, G. A. Grabowski, R. Aebersold and S. G. Withers (1994). Identification of Glu340 as the active-site nucleophile in human glucocerebrosidase by use of electrospray tandem mass spectrometry. *J Biol Chem* 269(15): 10975-10978.

Mie, M., F. Takahashi, H. Funabashi, Y. Yanagida, M. Aizawa and E. Kobatake (2003). Intracellular delivery of antibodies using TAT fusion protein A. *Biochemical and Biophysical Research Communications* 310(3): 730-734.

Mistry, P. K., E. P. Wraight and T. M. Cox (1996). Therapeutic delivery of proteins to macrophages: implications for treatment of Gaucher's disease. *Lancet* 348(9041): 1555-1559.

Morais, V. A. and J. Costa (2003). Stable expression of recombinant human alpha3/4 fucosyltransferase III in Spodoptera frugiperda Sf9 cells. *Journal of Biotechnology* 106(1): 69-75.

Morise, H., O. Shimomura, F. H. Johnson and J. Winant (1974). Intermolecular energy transfer in the bioluminescent system of Aequorea. *Biochemistry* 13(12): 2656-2662.

Morris, M. C., J. Depollier, J. Mery, F. Heitz and G. Divita (2001). A peptide carrier for the delivery of biologically active proteins into mammalian cells. *Nature Biotechnology* 19(12): 1173-1176.

Nagahara, H., A. M. Vocero-Akbani, E. L. Snyder, A. Ho, D. G. Latham, N. A. Lissy, M. Becker-Hapak, S. A. Ezhevsky and S. F. Dowdy (1998). Transduction of full-length TAT fusion proteins into mammalian cells: TAT-$p27^{Kip1}$ induces cell migration. *Nature Medicine* 4(12): 1449-1452.

Olsnes, S., O. Klingenberg and A. Wiedlocha (2002). Transport of Exogenous Growth Factors and Cytokines to the Cytosol and to the Nucleus. *Physiological Reviews* 83: 163-182.

Ong, E., N. R. Gilkes, R. C. Miller, Jr., A. J. Warren and D. G. Kilburn (1991). Enzyme immobilization using a cellulose-binding domain: properties of a beta-glucosidase fusion protein. *Enzyme Microb Technol* 13(1): 59-65.

Ong, E., N. R. Gilkes, R. C. Miller, Jr., R. Warren and D. G. Kilburn (1993). The Cellulose-Binding Domain (CBD_{cex}) of an Exoglucanase from *Cellulomonas fimi*:

Production in *Escherichia coli* and Characterization of the Polypeptide. *Biotechnology and Bioengineering* 42: 401-409.

Ong, E., J. Greenwood, N. R. Gilkes, D. Kilburn, R. J. Miller and R. A. J. Warren (1989). The Cellulose-binding Domains of Cellulases - Tools for Biotechnology. *Trends in Biotechnology* 7: 239-243.

Park, J., K.-A. Kim, J. Ryu, E. Y. Choi, K. S. Lee and S. Y. Choi (2000). Generation and characterization of cell-permeable green fluorescent protein mediated by the basic domain of Human Immunodeficiency Virus Type 1 Tat. *Journal of Microbiology and Biotechnology* 10(6): 797-804.

Patterson, G. H., S. M. Knobel, W. D. Sharif, S. R. Kain and D. W. Piston (1997). Use of the green fluorescent protein and its mutants in quantitative fluorescence microscopy. *Biophysical Journal* 73(5): 2782-2790.

Pfeifer, T. A. (1998). Expression of heterologous proteins in stable insect cell culture. *Curr Opin Biotechnol* 9(5): 518-521.

Pfeifer, T. A., M. M. Guarna, E. M. Kwan, G. Lesnicki, D. A. Theilmann, T. A. Grigliatti and D. G. Kilburn (2001). Expression analysis of a modified factor X in stably transformed insect cell lines. *Protein Expr Purif* 23(2): 233-241.

Pfeifer, T. A., D. D. Hegedus, D. A. Theilmann and T. A. Grigliatti (1997). Baculovirus immediate-early promoter-mediated expression of the Zeocin™ resistance gene for use as a dominant selectable marker in Dipteran and Lepidoteran insect cell lines. *Gene* 188: 183-190.

Pooga, M., M. Hallbrink, M. Zorko and U. Langel (1998). Cell penetration by transportan. *Federation of American Societies for Experimental Biology (FASEB) Journal* 12(1): 67-77.

Prasher, D. C., V. K. Eckenrode, W. W. Ward, F. G. Prendergast and M. J. Cormier (1992). Primary structure of the Aequorea victoria green-fluorescent protein. *Gene* 111(2): 229-233.

Princivalle, M. and A. de Agostini (2002). Developmental roles of heparan sulfate proteoglycans: a comparative review in Drosophila, mouse and human. *Int J Dev Biol* 46(3): 267-278.

Richard, J. P., K. Melikov, E. Vives, C. Ramos, B. Verbeure, M. J. Gait, L. V. Chernomordik and B. Lebleu (2003). Cell-penetrating peptides. A reevaluation of the mechanism of cellular uptake. *Journal of Biological Chemistry* 278(1): 585-590.

Rijnboutt, S., H. M. Aerts, H. J. Geuze, J. M. Tager and G. J. Strous (1991). Mannose 6-phosphate-independent membrane association of cathepsin D, glucocerebrosidase, and sphingolipid-activating protein in HepG2 cells. *J Biol Chem* 266(8): 4862-4868.

Rothbard, J. B., E. Kreider, C. L. VanDeusen, L. Wright, B. L. Wylie and P. A. Wender (2002). Arginine-rich molecular transporters for drug delivery: role of backbone spacing in cellular uptake. *Journal of Medicinal Chemistry* 45(17): 3612-3618.

Sambrook, J. and D. W. Russell (2001). *Molecular cloning : a laboratory manual.* Cold Spring Harbor, N.Y., Cold Spring Harbor Laboratory Press.

Sandvig, K. and S. Olsnes (1982). *Jounal of Biologial Chemistry* 257: 7504-7513.

Scheld, W. M. (1989). Drug delivery to the central nervous system: general principles and relevance to therapy for infections of the central nervous system. *Review of Infectious Disease* 11 Suppl 7: S1669-1690.

Schwarze, S. R. and S. F. Dowdy (2000a). In vivo protein transduction: intracellular delivery of biologically active proteins, compounds and DNA. *Trends Pharmacol Sci* 21(2): 45-48.

Schwarze, S. R., A. Ho, A. Vocero-Akbani and S. F. Dowdy (1999). In vivo protein transduction: delivery of a biologically active protein into the mouse. *Science* 285(5433): 1569-1572.

Schwarze, S. R., K. A. Hruska and S. F. Dowdy (2000b). Protein transduction: unrestricted delivery into all cells? *Trends in Cell Biology* 10: 290-295.

Seppo, A. and M. Tiemeyer (2000). Function and structure of Drosophila glycans. *Glycobiology* 10(8): 751-760.

Shimomura, O., F. H. Johnson and Y. Saiga (1962). Extraction, purification and properties of aequorin, a bioluminescent protein from the luminous hydromedusan, Aequorea. *J Cell Comp Physiol* 59: 223-239.

Silhol, M., M. Tyagi, M. Giacca, B. Lebleu and E. Vives (2002). Different mechanisms for cellular internalization of the HIV-I Tat-derived cell penetrating peptide and recombinant proteins fused to Tat. *European Journal of Biochemistry* 269: 494-501.

Sinclair, G. B. (2001). Mutation analysis, heterologous expression and characterization of human glucocerebrosidase. *Department of Biology*. Victoria, University of Victoria.

Sodroski, J., C. Rosen, F. Wong-Staal, S. Z. Salahuddin, M. Popovic, S. Arya, R. C. Gallo and W. A. Haseltine (1985). Trans-acting transcriptional regulation of human T-cell leukemia virus type III long terminal repeat. *Science* 227(4683): 171-173.

Staudacher, E., F. Altmann, I. B. Wilson and L. Marz (1999). Fucose in N-glycans: from plant to man. *Biochimica et Biophysica Acta* 1473(1): 216-236.

Strasberg, P. M., B. L. Triggs-Raine, I. B. Warren, M. A. Skomorowski, B. McInnes, L. E. Becker, J. W. Callahan and J. T. Clarke (1994). Genotype-phenotype pitfalls in Gaucher disease. *J Clin Lab Anal* 8(4): 228-236.

Suzuki, T., S. Futaki, M. Niwa, S. Tanaka, K. Ueda and Y. Sugiura (2002). Possible existence of common internalization mechanisms among arginine-rich peptides. *Journal of Biological Chemistry* 277(4): 2437-2443.

Takasaki, S., G. Murray, F. Furbish, R. Brady, J. Barranger and A. Kobata (1984). Structure of the N-asparagine-linked oligosaccharide units of human placental beta-glucocerebrosidase. *Jounral of Biological Chemistry* 259: 10112.

Terpe, K. (2003). Overview of tag protein fusions: from molecular and biochemical fundamentals to commerical systems. *Applied Microbiology and Biotechnology* 60: 523-533.

Theilmann, D. A. and S. Stewart (1992). Molecular analysis of the trans-activating IE-2 gene of Orgyia pseudotsugata multicapsid nuclear polyhedrosis virus. *Virology* 187(1): 84-96.

Theophilus, B., T. Latham, G. A. Grabowski and F. I. Smith (1989). Gaucher disease: molecular heterogeneity and phenotype-genotype correlations. *American Journal of Human Genetics* 45(2): 212-225.

Tomiya, N., D. Howe, J. J. Aumiller, M. Pathak, J. Park, K. B. Palter, D. L. Jarvis, M. J. Betenbaugh and Y. C. Lee (2003). Complex-type biantennary N-glycans of recombinant human transferrin from Trichoplusia ni insect cells expressing mammalian [beta]-1,4-galactosyltransferase and [beta]-1,2-N-acetylglucosaminyltransferase II. *Glycobiology* 13(1): 23-34.

Tomme, P., A. Boraston, B. McLean, J. Kormos, A. L. Creagh, K. Sturch, N. R. Gilkes, C. A. Haynes, R. A. J. Warren and D. G. Kilburn (1998). Characterization and affinity applications of cellulose-binding domains. *Journal of Chromatography B* 715: 283-296.

Tomme, P., N. R. Gilkes, M. Guarna, C. A. Haynes, D. Hasenwinkle, E. Jervis, P. Johnson, L. McIntosh, R. A. J. Warren and D. Kilburn (1996). Cellulose-binding domains: Versatile Affinity Tags for Inexpensive Large-Scale Purification, Concentration and Immobilization of Fusion Proteins. *Annals of the New York Academy of Science* 799: 418-424.

Tung, C. H., S. Mueller and R. Weissleder (2002). Novel branching membrane translocational peptide as gene delivery vector. *Bioorganic and Medicinal Chemistry* 10(11): 3609-3614.

Tyagi, M., M. Rusnati, M. Presta and M. Giacca (2001). Internalization of HIV-I Tat Requires Cell Surface Heperan Sulfate Proteoglycans. *The Journal of Biological Chemistry* 276(5): 3254-3261.

Van Weely, S., M. B. Van Leeuwen, I. D. Jansen, M. A. De Bruijn, E. M. Brouwer-Kelder, A. W. Schram, M. C. Sa Miranda, J. A. Barranger, E. M. Petersen, J. Goldblatt and et al. (1991). Clinical phenotype of Gaucher disease in relation to properties of mutant glucocerebrosidase in cultured fibroblasts. *Biochimica et Biophysica Acta* 1096(4): 301-311.

Varmus, H. (1988). Regulation of HIV and HTLV gene expression. *Genes and Development* 2(9): 1055-1062.

Vazquez, J., C. Sun, J. Du, L. Fuentes, C. Sumners and M. K. Raizada (2003). Transduction of a functional domain of the AT1 receptor in neurons by HIV-Tat PTD. *Hypertension* 41(3 Pt 2): 751-756.

Vendeville, A., F. Rayne, A. Bonhoure, N. Bettache, P. Montcourrier and B. Beaumelle (2004). HIV-1 Tat Enters T Cells Using Coated Pits before Translocating from Acidified Endosomes and Eliciting Biological Responses. *Molecular Biology of the Cell* 15(5): 2347-2360.

Violini, S., V. Sharma, J. L. Prior, M. Dyszlewski and D. Piwnica-Worms (2002). Evidence for a plasma membrane-mediated permeability barrier to Tat basic domain in well-differentiated epithelial cells: lack of correlation with heparan sulfate. *Biochemistry* 41(42): 12652-12661.

Vives, E., P. Brodin and L. Bernard (1997a). A truncated HIV-1 Tat protein basic domain rapidly translocates through the plasma membrane and accumulates in the cell nucleus. *Journal of Biological Chemistry* 272(25): 16010-16017.

Vives, E., C. Granier, P. Prevot and B. Lebleu (1997b). Structure activity relationship study of the plasma membrane translocating potential of a short peptide from HIV-I Tat protein. *Letters in Peptide Science* 4: 429-436.

Vocero-Akbani, A., M. A. Chellaiah, K. A. Hruska and S. F. Dowdy (2001). Protein transduction: delivery of Tat-GTPase fusion proteins into mammlian cells. *Methods in Enzymology* 332: 36-49.

Vocero-Akbani, A., N. A. Lissy and S. F. Dowdy (2000). Transduction of full-length Tat fusion proteins directly into mammalian cells: analysis of T cell receptor activation-induced cell death. *Methods in Enzymology* 322: 508-521.

Vocero-Akbani, A. M., N. Vander Heyden, N. A. Lissy, L. Ratner and S. F. Dowdy (1999). Killing HIV-infected cells by transduction with an HIV protease-activated caspase-3 protein. *Nature Medicine* 5(1): 29-33.

Vogel, B. E., S. J. Lee, A. Hildebrand, W. Craig, M. D. Pierschbacher, F. Wong-Staal and E. Ruoslahti (1993). A novel integrin specificity exemplified by binding of the alpha v beta 5 integrin to the basic domain of the HIV Tat protein and vitronectin. *Journal of Cell Biology* 121(2): 461-468.

Wassenberg, D., H. Schurig, W. Liebl and R. Jaenicke (1997). Xylanase XynA from the hyperthermophilic bacterium *Thermotoga maritima*: Structure and stability of the

recombinant enzyme and its isolated cellulose-binding domain. *Protein Science* 6: 1718-1726.

Weeks, B. S., K. Desai, P. M. Loewenstein, M. E. Klotman, P. E. Klotman, M. Green and H. K. Kleinman (1993). Identification of a novel cell attachment domain in the HIV-1 Tat protein and its 90-kDa cell surface binding protein. *Journal of Biological Chemistry* 268(7): 5279-5284.

Weeks, K. M., C. Ampe, S. C. Schultz, T. A. Steitz and D. M. Crothers (1990). Fragments of the HIV-1 Tat protein specifically bind TAR RNA. *Science* 249(4974): 1281-1285.

Weinreb, N. J., J. Charrow, H. C. Andersson, P. Kaplan, E. H. Kolodny, P. Mistry, G. Pastores, B. E. Rosenbloom, C. R. Scott, R. S. Wappner and A. Zimran (2002). Effectiveness of Enzyme Replacement Therapy in 1028 Patients with Type I Gacuher Disease after 2 to 5 Years of Treatment: A Report from the Gaucher Registry. *The American Journal of Medicine* 113(2): 112-119.

Wender, P. A., D. J. Mitchell, K. Pattabiraman, E. T. Pelkey, L. Steinman and J. B. Rothbard (2000). The design, synthesis, and evaluation of molecules that enable or enhance cellular uptake: peptoid molecular transporters. *Proceeding of the National Academy of Science U S A* 97: 13003-13008.

Wheeler, D. S., K. E. Dunsmore and H. R. Wong (2003). Intracellular delivery of HSP70 using HIV-1 Tat protein transduction domain. *Biochemical and Biophysical Research Communications* 301(1): 54-59.

Xia, H., Q. Mao and B. L. Davidson (2001). The HIV Tat protein transduction domain improves the biodistribution of beta-glucuronidase expressed from recombinant viral vectors. *Nat Biotechnol* 19(7): 640-644.

Xu, Y. H. and G. A. Grabowski (1998). Translational inefficiency of acid beta-glucosidase mRNA in transgenic mammalian cells. *Molecular Genetics and Metabolism* 64(2): 87-98.

Xu, Y. H., E. Ponce, Y. Sun, T. Leonova, K. Bove, D. Witte and G. A. Grabowski (1996). Turnover and distribution of intravenously administered mannose-terminated human acid beta-glucosidase in murine and human tissues. *Pediatric Research* 39(2): 313-322.

Yang, T. T., L. Cheng and S. R. Kain (1996). Optimized codon usage and chromophore mutations provide enhanced sensitivity with the green fluorescent protein. *Nucleic Acids Research* 24(22): 4592-4593.

Zhao, M. and R. Weissleder (2004). Intracellular cargo delivery using tat peptide and derivatives. *Medical Research Reviews* 24(1): 1-12.

Ziegler, A., X. L. Blatter, A. Seelig and J. Seelig (2003). Protein transduction domains of HIV-1 and SIV TAT interact with charged lipid vesicles. Binding mechanism and thermodynamic analysis. *Biochemistry* 42(30): 9185-9194.